DERIVATION OF PRINCIPAL STRAINS FROM DEFORMED BRACHIOPODS

by

CYRIL J. GALVIN, JR.

B.S., Saint Louis University
(1957)

SUBMITTED IN PARTIAL FULFILLMENT
OF THE REQUIREMENTS FOR THE
DEGREE OF MASTER OF SCIENCE
at the
MASSACHUSETTS INSTITUTE OF TECHNOLOGY
June, 1959

Signature of Author .....
Department of Geology and Geophysics, May 25

Certified by .....
Thesis Supervisor

Accepted by .....
Chairman, Departmental Committee on Graduate Students

DETERMINATION OF PRINCIPAL STRAINS FROM DEFORMED BRACHIOPODS

by

Cyril J. Galvin, Jr.

Abstract

It is possible to compute the magnitudes and directions principal strains from any fossil in which at least two of three mutually perpendicular lines remain recognizable after deformation. Ratios of lengths of these lines in deformed and undeformed fossils, and angular changes from the perpendicular of these lines in deformed fossils constitute the basic data. From Nadai's graphical representation of strain on the Mohr diagram this data yields the magnitude and direction of principal strains for a particular case of deformation. For the general case of deformation this theory approximately determines elongations in three, non-principal directions of each fossil.

The procedure is applied to the brachiopod Leptocoelia flabellites from folded Devonian rocks in northwestern Maine. Two determinations of principal strains indicate that the maximum strain axis approximately parallels the fold axis and the intermediate strain axis is perpendicular to the cleavage. Computations of non-principal elongations support these results.

Two strain axes lie in the plane of cleavage: the maximum strain axis (about 50% extension) parallel or sub-parallel with the fold axis, and probably the minimum strain axis (about 25% shortening) approximately perpendicular to the fold axis. Directions of principal strains indicated for Tarratine rocks are unlike published results in the literature, but further results are needed to verify this.

Strain is probably not homogeneous over a distance 15 meters along strike.

Thesis Advisor: W. F. Brace, Assistant Professor of Geology

TABLE OF CONTENTS

Text

TABLE OF CONTENTS (continued)

Figures

Plate

Tables

INTRODUCTION

The Problem

For more than a century, the geometry and genesis of folds in the earth's crust have been studied by structural geologists, but although much information has accumulated about their spatial distribution, there is little detailed knowledge of how folds develop. To understand the genesis of folds, geologists still lack basic geometric information about the character of strain involved in folding.

A fold is the final product of a long deformational history, but reconstruction of this history is impossible without an accurate knowledge of the original and intermediate states through which the deformed rocks have passed. If folded rocks contain objects whose original unstrained shapes are adequately known (for example, fossils), then at least the initial and final stages in this history can be learned, although the exact path between these stages is still ambiguous.

It is the purpose of this paper to compare the present strained state with the inferred undeformed state of 300 meters of sandstone and slate from the Tarratine formation on the southeastern limb of the Moose River synclinorium in northwestern Maine. This comparison between initial and final strain states is made possible by the frequent inclusion, in the sandstone, of shell beds containing many deformed

specimens of the brachiopod Leptocoelia flabellites, whose original shape is known from collections in undeformed areas. By measuring changes in shape of the deformed Leptocoelia, this study attempts to show quantitatively the finite geometric changes introduced into these rocks by folding.

In particular, this study tries to determine: 1) the strain at given localities; 2) the size of the region over which strain is homogeneous; 3) the variation in strain along and across a minor fold on the limb of the synclinorium.

Like the ordinary structural field investigation, this is a study of the geometry of deformed rocks, but it differs by being more quantitative and on a very small scale. Also like the ordinary field investigation, the results are strictly applicable only to the area studied. And since this is a study of geometric changes only, the results are insufficient to describe the nature of the deforming forces.

However, it is reasonable to assume that folded rocks elsewhere in the crust of the earth will show similarities to those in northwestern Maine, and that the forces which produce these folds do have some relationship to the amount and type of strain produced. Thus it is hoped that the results of this study will indicate qualitatively how folding in general might have occurred, as well as describe quantitatively how it did occur in a small area in northwestern Maine.

Acknowledgements

W. F. Brace, Assistant Professor of Geology at Massachusetts Institute of Technology, suggested this study and supervised the work. The application of the theory of finite strain to deformed fossils, and the design of the goniometer and strain gage are due largely to Brace. The writer is also indebted to Brace for aid in collecting oriented samples of fossils near Tarratine, Maine, and for critically reviewing earlier versions of this paper.

A. J. Boucot, Assistant Professor of Geology at Massachusetts Institute of Technology, suggested the suitability of the Tarratine locality for this study, aided in paleontologic problems, suggested the use of the goniometer, and read part of the manuscript.

Permission to measure steinkerns of Leptocoelia flabellites from the Camden chert collection at the United States National Museum was obtained from G. A. Cooper. The steinkerns from the Highland Mills member of the Esopus formation were supplied by Boucot. Permission to borrow and measure steinkerns from the Shaler collection at the Museum of Comparative Zoology of Harvard was obtained from H. D. Whittington.

Richard Maehl and John Griffin, geology students at Massachusetts Institute of Technology, suggested the inter-

pretation of cleavage-bedding relationships at the Tarratine railroad cut.

This study was supported by a grant, to Brace, from the Geological Society of America.

The opportunity to make this study under active supervision and with adequate facilities is gratefully acknowledged.

Outline of Investigation

This paper begins with a review of previous studies of finite strain in fossils, ooids, and pebbles. The second section describes the structure and stratigraphy of the rocks southeast of Tarratine, Maine from which fossils used in this study were collected.

These fossils, the steinkerns of Leptocoelia flabellites, are described, and the parameters selected for measurement are defined. Measurements of Leptocoelia steinkerns from rocks of Tennessee, New York, and Quebec are presented to show the natural variation of the parameters as a function of the size of the steinkern. The method of collecting, preparing, and measuring the steinkerns is described.

The theory of finite strain, graphically illustrated by Mohr diagrams, is used to analyze the data obtained from measuring Tarratine steinkerns. The state of strain thus determined for Tarratine steinkerns is compared with results obtained by previous investigators in different areas using different geologic strain gages. Possible errors in measurement, and the validity of assumptions necessary for this study are discussed.

Symbols used in this paper are summarized in the appendix.

HISTORICAL REVIEW

Deformed Fossils

The previous application of deformed fossils to the study of strained rocks, and the analogous use of stretched pebbles and ooids is here briefly outlined. For ease of comparison, the conclusions of principal studies are presented in Table I.

Wherever possible in Table I, the maximum, intermediate, and minimum axes ($\sqrt{\lambda}_1$, $\sqrt{\lambda}_2$, $\sqrt{\lambda}_3$) of the strain ellipsoid are listed, and their directions in a,b,c coordinates are given. a is assumed to be the dip direction of cleavage, b the axial direction of folds, and c the normal to cleavage. The particular object whose strain was measured, the type and age of rock from which it came, and the geographic location of the rocks are also listed wherever possible.

The information for some of the studies, particularly those in French, has been obtained from reviews by Cloos (1947), Rutsch (1949), Bucher (1953), and Breddin (1956a).

Table I. Strain Measurements in Rocks

In most cases, a is the dip direction of cleavage, b is the direction of the fold axes, and c is normal to the cleavage. Direction of tectonic transport is not implied. $\sqrt{\lambda}_1$, $\sqrt{\lambda}_2$, $\sqrt{\lambda}_3$ are the maximum, intermediate, and minimum axes of the strain ellipsoid. Where not otherwise stated, values have been computed from averages of the original data. References not examined first hand are marked by an asterisk. This table includes many of the important papers on strain measurements, but it is not a complete bibliography of the subject.

Reference	Strain Ellipsoid axes and directions $\sqrt{\lambda_1}$ $\sqrt{\lambda_2}$ $\sqrt{\lambda_3}$	geologic strain gage	rock age and lithology	location
Phillips, 1844	no measurements; $\sqrt{\lambda_1}$ in b?	brachiopods, trilobites, algae	slates, and flagstones	North Devon
Sharpe, 1847	1.5 ± ? in a 1 in b <1 in c	spirifers trilobites	slates U. Dev.?	Tintagel Petherwin
Sorby, 1853*, 1908	1.6 in a 1.0 in b 0.27 in c (recomputed Cloos, 1947, p. 847)	spots in Welsh slates	slates	Wales
Haughton, 1856	1.79 in b 1.64 in a .44 in c	spirifers trilobites	slates, Sil. and Carboniferous	8 loc. including Tintagel & Petherwin
Dufet, 1875*	$\sqrt{\lambda_1} = \sqrt{\lambda_2}$ in plane of shistosity $\sqrt{\lambda_3}$ perpendicular to shistosity (Breddin, 1956a, p. 239)	trilobites	shist	
Wettstein, 1886*	$\sqrt{\lambda_1} \approx 2\sqrt{\lambda_2}$ $\sqrt{\lambda_1}$ in a $\sqrt{\lambda_2}$ in b (Heim, 1921, p. 89)	fish skeletons	shists, chalks Oligocene	Kanton Glarus, Switz.
Chapman, 1893*	1.4 1 .7 - average 3 1 .3 - extremes (Cloos, 1947)	ooids	limestone	Ilfracombe

Reference	Strain Ellipsoid axes and directions $\sqrt{\lambda}_1$	$\sqrt{\lambda}_2$	$\sqrt{\lambda}_3$	geologic strain gage	rock age and lithology	location
Sieburg, 1909* Loretz, 1882*	$\sqrt{\lambda}_1$ & $\sqrt{\lambda}_2$ in cleavage plane (Cloos, 1947)			ooids	limestone	Thuringia
Heim, 1921	1.6 2.9	.79 .58	.79 .58	fossils, pebbles and ooids	varied lithogies Cret. and Jurassic	Switzerland
	$\sqrt{\lambda}_1 > 10$ for some intensely deformed rocks (Cloos, 1947)					
Runner, 1934	$\sqrt{\lambda}_1$ in b	$\sqrt{\lambda}_2$ in a	$\sqrt{\lambda}_3$ in c	pebbles	conglomerate Pre-Cambrian	Black Hills
Fairbairn, 1937	$\sqrt{\lambda}_1$ in b	$\sqrt{\lambda}_2$ in a	$\sqrt{\lambda}_3$ in c	quartz pebbles	conglomerate Pre-Cambrian	Patricia District, Ontario
Mehnert, 1939*		$\sqrt{\lambda}_2 = 8\sqrt{\lambda}_3$		coarse quartzite	Meta conglomerate	Saxony
		$\sqrt{\lambda}_2 = (10 \text{ to } 12)\sqrt{\lambda}_3$		dense graywacke		
		$\sqrt{\lambda}_2 = 18\sqrt{\lambda}_3$		shistose graywacke & shales		
		(Cloos, 1947)				
Strand, 1944 Goldschmidt 1916*	2.7 2.6	.83 .87	.46 in c .43	quartzite boulders and cobbles	quartzite cong. Eo-Cambrian	Southcentral Norway

Reference	Strain Ellipsoid axes and directions $\sqrt{\lambda}_1$	$\sqrt{\lambda}_2$	$\sqrt{\lambda}_3$	geologic strain gage	rock age and lithology	location
Kvale, 1945	7.5	1.2	.12	quartzite pebbles	quartzite conglomerate	Bergen, Norway
	$\sqrt{\lambda}_1$ parallel lineation based on a 2:1:1 ellipsoid					
Cloos, 1947	1.45 in a	1.05 in b	.66 in c	ooids	oolites Cambrian Ordovician	Maryland, Pennsylvania
	average value					
Oftedahl, 1948	2.0	1.2	0.42 in c	pebbles	conglomerate Eo-Cambrian	Central Norway
	no folding say Oftedahl $\sqrt{\lambda}_1$, $\sqrt{\lambda}_2$ in cleavage plane based on sphere					
Flinn, 1955	2.1 in b	.97 in a	.48 in c	quartzite pebbles	conglomerate pre-Old Red ss.	Shetland Islands
	based on sphere					
Elwell, 1955	3.5 in b	0.9 in a	.3 in c	ss. & granitic cobbles	conglomerate Dalradian	County Mayo
	based on sphere					
Hellmers, 1955	1.06	1.06	.85 in c	crinoid plates	sandstones L. & M. Dev.	rh. Schieferge-birge
	computed by Breddin, 1957					
Breddin, 1956b	i 1.35	1.35	.85 in c	brachiopods, pelecypods, trilobites, crinoid plates, cephalopods	shales; slightly sandy shales; sandy shales, gray-wacke Devonian and Carboniferous	i most of rh. Schiefergebirge
	ii 1	1	.85 in c			ii Karbongurtel
	iii 2.0 in a	1.3 in b	.35 in c			iii Venmassiv

Recognition of deformed fossils occurred at least as early as 1814 (Bucher, 1953, p. 276). In 1829, De la Beche used the existence of belemnites in garnetiferous mica shist of the Alps to disprove the Wernerian idea that metamorphic rocks are, a priori, the geologically most ancient rocks.

About the same time, fossils were identified in metamorphic rocks of Massachusetts by Edward Hitchcock (1835), and later they were found in metamorphics of the Urals, Brittany, Norway, Venezuela, and elsewhere. The history of the discovery of fossils in metamorphic rocks is thoroughly reviewed by Bucher (1953).

Early descriptive study of deformed fossils was concerned with proving the fossils' existence, and establishing the sedimentary origin of some metamorphic rocks. This study continued through the 19th century, and in modified form, still continues at present (Boucot, et al, 1958).

The importance of deformed fossils as measurements of strain in rocks was recognized by British geologists in the middle of the 19th century. Possibly the first recorded use of deformed fossils to measure strain is a comment by Phillips (1844, p. 61) that "in the space occupied by a trilobite, it [the change in length] amounts to a quarter, or even half an inch." The author interprets Phillips' brief paper to indicate maximum extension parallel to the strike of cleavage in b. Phillips suggests that fossil deformation might be

useful in explaining the origin of cleavage.

Three years later, Sharpe (1847) made the following conclusions from a study of the relations between deformed spirifers and trilobites, and slatey cleavage: 1) maximum shortening is perpendicular to planes of cleavage, 2) maximum extension is in the direction of dip of cleavage, and 3) in the direction of strike of cleavage, there is no evidence for change in length. No measurements are given. Later, Sharpe (1849) supported his conclusions with evidence from deformed spots in slates.

These "spots in Welsh slates" were shortly afterwards investigated by Sorby (1853) who furnishes the first quantitative measurements of deformation, shown in Table I. By making assumptions concerning volume change and the intermediate axis of strain, Sharpe's conclusions are quantitatively confirmed. Much later in a paper based on this 1853 work, but published posthumously in 1908, Sorby makes the earliest attempt known to the author to calculate volume change due to deformation.

Haughton applied Cauchy's ellipsoid to the study of deformed fossils, including some of the same specimens studied previously by Sharpe (Haughton, 1856, p. 415), but he got different results. The measurements, averaged in Table I, indicate that maximum extension is usually parallel to the strike of cleavage, and rarely parallel to the dip of cleavage as Sharpe had concluded. The difference between maximum and

intermediate axes of strain, $\sqrt{\lambda}_1$ and $\sqrt{\lambda}_2$, is small. For some reason, Haughton does not mention Sorby's earlier study on slate spots.

During the last quarter of the 19th century, European geologists, including Dufet (1875), Daubree (1876, 1879), Albert Heim (1878, 1921), Janettaz (1884) and others, studied the relation of deformed fossils to shistosity and cleavage.

Heim's encyclopedic study of Swiss geology included observations on deformed pebbles, oolites, and fossils, particularly the use of belemnites in determining direction and amount of strain. Some of his results are included in Table I.

Hellmers (1955) applied Cloos' oolite technique (see below page 22) to the limited two dimensional problem of crinoid columnals in a bedding plane. His study showed that the magnitude of maximum strain in the bedding plane decreased systematically across the rheinische Schiefergebirge, and that the direction of maximum strain varied from parallel to fold axes in one region to independent of fold axes in another region.

At the time Hellmers published his paper, the problem of crinoid columnal deformation in the same region was being investigated by Hans Breddin as part of his extensive study of fossil deformation in the rheinische Schiefergebirge (Breddin, 1957, p. 334). There is some disagreement between

the quantitative values of strain, but both studies agree in the direction of strain increase.

Breddin's recent papers include a detailed presentation of the theory of finite strain applied to deformed fossils (1956a) and an application of this theory to regions about the Schiefergebirge (1956b, 1957).

Strain is measured in brachiopods, pelecypods, cephalopods, trilobites, and crinoids. Measurements are taken in the bedding plane to eliminate distortion due to compaction from the weight of overlying sediments.

Breddin assumed that the cleavage plane contains the direction of maximum and intermediate extension, and that generally maximum shortening is perpendicular to this plane. Volume changes due to tectonic deformation are assumed to be 15, 10, 5, and 0% for shale, slightly sandy shale, sandy shale, and sandstone respectively. It is emphasized that strain in fossils gives a minimum value for strain in the inclosing rocks.

Numerous measurements of varied fossil types from widespread localities in the Schiefergebirge indicate that deformation has been accomplished by shortening perpendicular to the cleavage, and equal extension in all directions parallel to the cleavage. Exceptions to this rule are the Karbongurtel rocks where deformation was accomplished by shortening perpendicular to the cleavage without corresponding extension in the plane of the cleavage, and rocks of east Sauerland where

extension in the dip of cleavage exceeds extension parallel to the strike of cleavage. Save for this last example, deformation in the rheinische Schiefergebirge is characterized by a strain ellipsoid of rotation whose equator lies in the plane of cleavage.

Deformation in fossils supplies constructive information to the structural geologist, but to the paleontologist such deformation causes taxonomic confusion. Occasionally plates figured by paleontologists exhibit obviously deformed specimens (Dawson, 1855, p. 317, fig. 35c; Barrande, 1852, plates 31, 35, 36; Hall, 1859, pl. XLVII, fig. 8), but because deformed fossils have doubtful value for classification, such pictures are infrequent. But when the fossil has no original symmetry, or when elongation parallels a direction of original symmetry, the undetected distortion of lengths and angles may lead to the establishment of new, but imaginary, species.

As an example of this, Crickmay (1933, p. 52) desdribes how Hyatt unwittingly set up pelecypod "species" whose specific differences were established, not by inherited characteristics, but by orientation of the shell with respect to the directions of strain.

Another example is the Oligocene fish collection from the Glarnerschiefer beneath the Glarus overthrust in Switzerland. Originally the fish skeletons were classified into 13 species by Agassiz. Later, Wettstein (1876) was able to

show, by applying the theory of plane finite strain, that most of Agassiz "species" had identical shapes when the effects of deformation were removed.

Most paleontologists do not discuss the problem of removing the effects of deformation, but they frequently mention deformed specimens (Elles, 1944; Imlay, 1939, and many others). Lake (1943) suggests a photographic technique of removing strain. Some fossils, such as deformed Scolithus (Wanner, 1890), or ostracods (Johnson, 1936, p. 8), would be valuable geologic strain gages for future study because of their simple geometry.

Deformed Ooids

The simplest of all original shapes for the study of strain is a sphere, and in common deformed rocks, the nearest approach to spheres are ooids (defined as in Cloos, 1947). Loretz (1882) and Sieburg (1909) studied Thuringian oolitic limestones, and noted that maximum and intermediate extensions lie in the cleavage plane. Chapman (1893) observed deformed oolites at Ilfracombe. Heim (1921) pictures deformed ooids.

Ernst Cloos (1947) used deformed ooids in a thorough study of strain in folded rocks. In this study, thin sections were cut on mutually perpendicular planes in oriented oolite samples collected from known localities on the recumbent South Mountain fold. By assuming that the ooids had been originally spherical, and that no volume change had occurred,

strain was calculated from the elliptical outlines of the deformed ooids.

Regional oolite deformation was found to vary continuously across South Mountain, reaching a maximum in the lower limb. Locally, strain varies unsystematically in small folds (p. 881), or in parts of the major fold (p. 880). The average maximum strain axis is 1.36 on the upper limb and 1.56 on the overturned lower limb.

Without exception the maximum and intermediate strain axes, $\sqrt{\lambda}_1$ and $\sqrt{\lambda}_2$, lie in the plane of cleavage, and the least strain axis, $\sqrt{\lambda}_3$, normal to it. Cleavage attitude varies with position on the fold, forming a fan opening to the southeast which is the direction of overturning.

$\sqrt{\lambda}_1$, or the maximum strain, is oriented in the dip of cleavage in almost all cases. Extension has occurred parallel with the fold axes (in b), but it is usually very small. Linear structures, the presence or absence of cleavage, or intensity of folding show no relation to extension in b.

Stretched Pebbles

Besides ooids, pebbles are common subspherical components of deformed rocks, but for pebbles, the original shape is less certainly spherical.

Stretched pebbles are reported at least as early as 1861 (Hitchcock, et al, vol. I, p. 28-45), but unlike the

study of deformed fossils, most pebble investigations are relatively recent, and have been carried out by structural petrologists in an effort to correlate grain orientation with macroscopic features. The relationship of pebble elongation to grain orientation and the direction of tectonic transport has recently been critically discussed by Turner (1957), but the subject cannot be reviewed here.

Pebbles with their long axes parallel with fold axes have been noted by Fairbairn (1937), Cloos (1936), and Runner (1934). Fairbairn and Runner both report that local geologic evidence indicates that the pebbles were deformed only once.

Kvale (1945) measured greatly elongated pebbles from east of Bergen. Strand (1945) studied the Bygdin conglomerate which had previously been investigated by Goldschmidt (1916). Kvale and Strand both found the long axes of pebbles parallel with the axes of minor folds, but in both studies the direction of tectonic transport was also interpreted to lie parallel with these folds.

Oftedahl (1948) made a regional study of deformed quartz conglomerates in central Norway including samples from the Bygdin conglomerate of Strand's study. It is reported that the rocks have not been folded. By making the usual assumption of no volume change and an original spherical shape for the pebbles, it is shown that strain is three dimensional.

In a study of quartzite pebble deformation in central Vermont, Brace (1955) found that the long axes of pebbles are subnormal to fold axes, a condition which has not been observed regionally in any other work known to the author. Adjoining pebbles had radically different fabric diagrams, and no correlation was found between the intensity of maxima, and extension of pebbles. Brace suggested that some of the fabric is residual from earlier deformation.

Flinn (1956) describes the rapid increase of deformation away from a thrust fault in the Funzie conglomerate of the Shetland Island. The long and intermediate axes of pebbles lie approximately in the plane of shistosity. Pebbles are elongated parallel to the strike of shistosity or lineation in the north, and about 40° from the strike of shistosity in the south of the area studied.

Ewell (1955) describes flattened and elongated cobbles from the Dalradian of Mayo, and concludes that they have been elongated in b by rolling. Deformation varies widely in neighboring outcrops.

Mehnert (1939) demonstrated the relation between deformation and composition of pebbles. That quartzite pebbles are less deformable than graywacke pebbles, and graywacke pebbles are less deformable than shistose graywacke, as Mehnert showed, may seem intuitively obvious, yet the study is valuable because it indicates that, in at least some cases, the relative strengths of different pebble compositions under

ordinary surface conditions of temperature and pressure retain the same relationships under the extraordinary conditions of diastrophism.

Summary of Previous Work

The accumulated values for both magnitude and direction of principal strain axes are apparently contradictory. Much of the apparent confusion may result from differences in geologic history of the areas investigated, differences in composition of the material investigated, differences in assumptions and methods of investigations, and finally differences in personal prejudices of the investigators. There are, however, tentative conclusions to be drawn from the work reviewed above.

Examination of Table I indicates that both direction and magnitude of maximum elongation $\sqrt{\lambda}_1$ can be correlated with the particular geologic strain gage used for measurements. Almost all studies of stretched pebbles find $\sqrt{\lambda}_1$ parallel to fold axes, but almost all studies of deformed fossils and ooids find $\sqrt{\lambda}_1 = \sqrt{\lambda}_2$, or $\sqrt{\lambda}_1$ perpendicular to fold axes. Similarly, it is obvious that strain in quartzose pebbles is surprisingly greater than in calcareous fossils and ooids. Possibly this second correlation results from too much strain obliterating the fossils and ooids used to measure it.

Also from Table I, there seems to be a slight, but

probably accidental correlation between age and the lithology of the rock whose strain has been investigated. In part this is due to the late arrival of fossils in the geologic column.

Although their directions and magnitudes differ, $\sqrt{\lambda}_1$ and $\sqrt{\lambda}_2$ are always reported to lie in the plane of cleavage, or shistosity. $\sqrt{\lambda}_3$ is normal to the $\sqrt{\lambda}_1$ $\sqrt{\lambda}_2$ plane. The relation between strain axes and cleavage or shistosity is important in any theory of origin of these features, but it is not apparent from the literature whether the $\sqrt{\lambda}_1$ $\sqrt{\lambda}_2$ plane is identical to, or only closely approximated by the plane of cleavage or shistosity.

Regional studies of Cloos, Flinn, Breddin, Hellmers, Strand, and Oftedahl show continuous, systematic variations of average strain which can be correlated with geologic structures, but the variation at any given locality is often unsystematic.

Elwell reported extremely unsystematic variation from the Dalradian of County Mayo where outcrops of subspherical cobbles adjoin outcrops of intensely stretched and flattened cobbles (see Table I). In the Funzie conglomerate, Flinn found that the range of strain in pebbles from any given locality often exceeded the range of average strain for all the localities studied. Oolite deformation shows surprising variation in some of Cloos' cross sections.

Thus on a regional scale, strain varies continuously, but within any small area, wide variations can be expected. It seems logical to conclude that strain may be concentrated in individual beds. It also seems logical to assume that the number of fossils, ooids, or pebbles to be measured at any locality should be statistically determined.

The principal points emphasized in the above discussion are as follows:

1) for pebbles, $\sqrt{\lambda}_1$ usually parallels fold axes, but for fossils and ooids, $\sqrt{\lambda}_1 = \sqrt{\lambda}_2$ or $\sqrt{\lambda}_1$ is perpendicular to fold axes.
2) maximum strain in quartzose pebbles is usually greater than maximum strain in calcareous fossils and ooids.
3) the $\sqrt{\lambda}_1$ $\sqrt{\lambda}_2$ plane is parallel with, and the $\sqrt{\lambda}_3$ direction is perpendicular to cleavage or shistosity.
4) strain varies systematically on a regional scale, but often is discontinuous on a local scale.

It is important to remember that the work reviewed above is based on assumptions that are not always explicitly stated. Volume change is given some arbitrary value, usually zero. An original shape for the strained object must be assumed. Often the intermediate strain axes is arbitrarily determined. Strain in the fossil, ooid, or pebble is assumed to be a minimum, but reasonably close, value for

strain in the inclosing rock. Deformation is supposed to be mathematically comparable to the deformation of a sphere into an ellipsoid.

Presumably, the reliability of a strain measurement is inversely proportional to the number of assumptions used in making the measurement. The number and the validity of the assumptions necessary for computing strain in deformed Leptocoelia is discussed in a later section of this paper.

GEOLOGY OF THE AREA SOUTHEAST OF TARRATINE, MAINE.

The Tarratine Formation

The deformed fossils studied in this report were taken from shell beds included in the Tarratine formation exposed along the Canadian Pacific railroad, one mile southeast of Tarratine, Brassua Lake Quadrangle, Somerset County, Maine.

These outcrops are in the basal third of the type section of the Tarratine formation as defined by A. J. Boucot (in preparation). The Tarratine forms the base of the Lower Devonian Moose River group, and it is equivalent in age to the Oriskany sandstone of New York.

Possibly because of local sediment sources, the formation as a whole is highly variable in thickness and individual beds lens out quickly among strike. Maximum thickness reaches 10,000 feet (A. J. Boucot, in preparation), but along the railroad southeast of Tarratine, thickness is 4200 feet (unpublished map by Joyner and B. Boucot, 1950).

The dominant part (80 to 85%) of the Tarratine formation studied in this paper is fine to medium grain-sized, well indurated, quartzitic sandstone (subgraywacke) which crops out in brown to gray beds ranging from a centimeter to a meter in thickness. Where freshly exposed, the sandstone crops out in massive, dark blue-gray beds which appear at first glance to be many meters thick, but which actually are composed of thinner units less than a meter in thickness.

None of the individual beds are persistent stratigraphic units, and some are contained within the width of a single outcrop. In this study of finite strain, slip along the bounding surfaces of these intertonguing sandstone beds must be considered as a possible method of strain adjustment. However, slickensides on these surfaces were not observed, except near a few minor reverse faults.

Some massive beds show faint laminations of alternating dark and less dark sandstone, usually parallel to the bedding, or at a low angle as shallow crossbedding. One massive bed near the base of the formation contained several contorted sandstone rolls about 15 centimeters in diameter.

Where the sandstone is thin bedded, it frequently alternates with lenses of siltstone and slate. These latter rock types make up to 15 to 20% of the lower Tarratine, and only about 10% of the Tarratine formation as a whole. The slate is gray to brown on the weathered surface and dark gray

where fresh. The siltstone weathers to a rusty brown and typically has an angle between cleavage and bedding greater than the slate, but less than the sandstone.

The occurrence of even this relatively small percentage of slate with the sandstone puts an important limitation on this study of finite strain, for according to a classic concept of structural geology, the slate is more incompetent than the sandstone, and thus a disproportionately large amount of strain might be concentrated in relatively few beds of the fold. However, as the slate occurs as thin lenses in the sandstone and not as continuous beds across the fold, this possibility may be considerably lessened.

Shell Beds

The most significant feature of Tarratine lithology for this study is the concentrations of fossil brachiopods. Seventeen separate shell concentrations were found across the strike of the lower Tarratine formation along the Canadian Pacific right of way southeast of Tarratine, Maine. These concentrations varied from a few dozen scattered shells sprinkled on a bedding surface of the sandstone, to distinct, lenticular shell beds up to 20 centimeters thick and several meters long.

In the shell beds, fossil brachiopods, together with discoid slate pebbles up to five centimeters long, are packed in a sandstone matrix similar to the ordinary Tarratine sand-

stone described above. After investigating several possibilities, the internal casts, or steinkerns, of articulated specimens of Leptocoelia flabellites contained in these shell beds were selected for measurement of strain.

Except for a few small individuals composed of clay-sized fragments, the material of the steinkerns does not differ in grain size or composition from the surrounding matrix. This similarity of steinkern and matrix lithology is necessary if the strain of the surrounding rocks is to be validly described by the strain of the inclosed steinkerns.

A study of thin sections and polished sections of shell beds indicates that the fossil concentrations contain as much as 15 percent carbonate shell material. This high percentage of relatively ductile carbonate shell material suggests the possibility of strain concentration in these beds similar to that discussed above for slate (page 32). However, the fact that fossils still exist in easily recognizable form indicates that strain concentration in the calcite, if it occurred at all, was not great. Moreover, experimental work by Handin (personal communication, 1958) indicates that calcite and quartz deform uniformly in a calcite-cemented quartz sandstone.

The paleoecology of these shell beds is a subject distinct from this study and it has been treated elsewhere (Boucot, Brace, and DeMar, 1958; Boucot, in preparation). However, it is interesting to note that, of the 17 fossil

concentrations encountered, 8 occur just above slate or siltstone at the base of a thickbedded sandstone sequence. Four of the 17 occur in sandstone lenses isolated in slate or siltstone, and two others occur in interbedded sandstone and slate. Only three of the 17 lenses occur more than 0.5 meters above slate or siltstone in thickbedded sandstone.

All fossil beds have a sandstone matrix, and most of them are found in, or immediately above, the fine clastic material which makes up less than 20% of the total section. It would seem unlikely that this observed correlation between fossil concentrations and a position immediately above or within fine clastic material is due to chance. This correlation is probably true for the formation as a whole, for most of the fossils are from the lower Tarratine where the percentage of fine clastic sediments is greatest.

Perhaps the fossils inhabited shallow, muddy sea floors, and were swept together, along with mud pebbles, into lenses as the environment shifted from one of mud deposition to one of sandstone deposition. The consistent position of shell beds in sandstone above slate and siltstone would at least suggest this possibility.

Structural Geology

The slates, siltstones, and fossiliferous sandstones studied in this report are on the steep southeastern limb of the Moose River synclinorium, which is a major structural

element of the northern Appalachians, extending 60 miles in a northeast direction through northern Somerset County and adjacent parts of Piscataquis and Franklin Counties, Maine (Boucot, in preparation).

The steep southeast limb and the more gentle northwest limb of the synclinorium contain many assymmetric, doubly plunging anticlines, one of which is exposed in the outcrops southeast of Tarratine (unpublished map by Joyner and B. Boucot, 1950). The northeast limb of this anticline dips steeply toward the synclinorium axes, and the other limb dips gently to the southeast for 300 meters, interrupted by several higher order folds, before returning to the steep northwesterly dip of the synclinorium limb. See Plate I. Stereonet plots of cleavage and bedding shown in Figure 1 on page 37 indicate that the fold does not plunge in the area studied.

It is unlikely that the major synclinorium and its minor folds originated simultaneously; rather it is more probable that the minor folds developed after the major fold. Therefore, because the data used in this study were obtained from positions on minor (higher order) folds, the strain recorded in deformed Leptocoelia may be the result of two distinct sets of strain directions. This might be expected near location A in Plate I where the shearing sense of the minor fold may be opposite that of the major fold.

At least eight minor reverse faults cut thick-bedded

Figure 1. Poles to bedding, joints, cleavage, and faults in the Tarratine formation southeast of Tarratine, Maine. Lower hemisphere projection, north at top.

a average of 11 measurements of slate cleavage at C
b one sandstone cleavage at E
c average of eight faults at E
d average of 21 measurements of sandstone cleavage at C
e average bedding at E
f average of 14 measurements of slate cleavage at E
g average bedding at C
O joints at C
x joints at E

Locations of C and E are shown on Plate I inside rear cover.

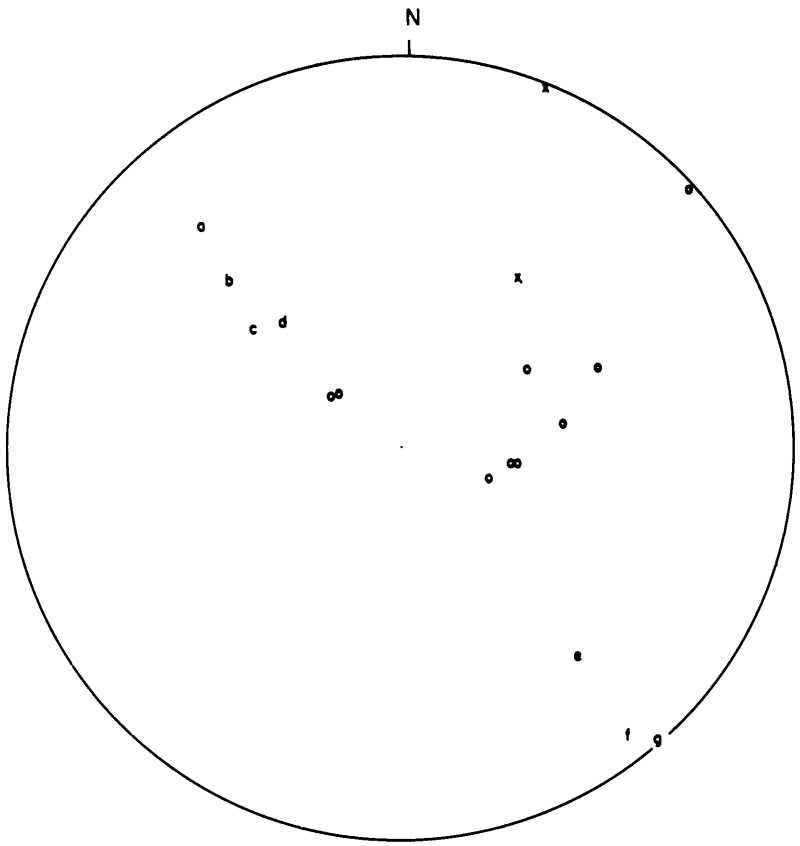
N
a
b
c
d
e
f
g

sandstone between 100 and 150 meters above the base of the Tarratine formation. These faults strike parallel to bedding and fold axis and dip 45° to 60° southeast. The maximum observable stratigraphic throw is less than four meters on all faults with the exception of one which has a minimum stratigraphic throw of four meters.

The rocks contain cleavage whose strike approximately parallels the fold axes, but whose dip varies with position on the fold and with the lithology of the rocks. A total of 47 cleavage orientations were measured at two localities. At locality C on the vertical northwest limb of the anticline, 21 measurements in sandstone and 11 in slate yield average angles between cleavage and bedding of 42° and 15° respectively. At locality E where the beds regain the normal dip of the synclinorium limb, 14 measurements in slate yield an average angle of 15° between cleavage and bedding. At E cleavage in sandstone is rare, and the only two measurements of the angle between cleavage and bedding were 42° and 48°.

Figure 1 on page 37 shows poles to cleavage and bedding at localities C and E. Between C and E, cleavage fans slightly across the crests of minor folds.

The constant angle between cleavage and bedding in slate, and probably in sandstone, at C where beds dip vertically and at E where beds dip 65° to 75° suggests that the cleavage may antedate the development of minor folds on the limb of the synclinorium.

In Figure 1, the poles to sandstone cleavage and the eight minor thrust faults fall in the same region, indicating that the faults might have developed by shearing along pre-existing cleavage surfaces.

There are at least two, and possibly three sets of joints, one of which is perpendicular to the fold axes and the other (or others) which parallels the fold axes, but they were not extensively studied. See Figure 1.

All rocks examined had undergone low-grade metamorphism. No igneous rocks crop out in the immediate vicinity of the fossil localities studied.

Tectonic History

Following Taconic diastrophism, thick sequences of Silurian and early Devonian rocks were deposited in northwestern Maine. The rapid changes in thickness and lithology of these sediments within short distances suggest their deposition in a tectonically mobile environment. (A. J. Boucot, in preparation).

Subsequent to their deposition, the Silurian and early Devonian rocks were strongly deformed by Acadian diastrophism during middle Devonian time. No record remains of the post-Acadian, pre-Pleistocene history of the Moose River synclinorium, and there is no evidence that late Paleozoic deformation affected this area.

For lack of evidence to the contrary, the strain studied in this report is assumed to be the product of one period of deformation (Acadian).

METHOD

Leptocoelia Flabellites

Description. To experimentally measure strain resulting from a given state of stress, an engineer can tape strain gages on the material to be tested, and then measure the change in length after the stress has been applied. For the geologist the problem is more difficult. The stress state which produced a given strain is unknown, and geologic strain gages are scarce and uncertain.

In this study of strain distribution in folded rocks, the steinkern (internal cast) of the brachiopod Leptocoelia flabellites is the geologic strain gage. The original dimensions of the deformed Leptocoelia are indicated by collections from undeformed regions.

Information for the following description of Leptocoelia was supplied by A. J. Boucot. It is not intended as a paleontologic description but as a precise definition of the parameters chosen for measurement, and an explanation of the reasons for the choice. The necessary morphologic terminology can best be understood by referring to Figure 2.

Over a century ago, Conrad (1841) and Hall (1859) described Leptocoelia flabellites from the Lower Devonian of New York State.

Similar to nearly all brachiopods, Leptocoelia has

Figure 2. Leptocoelia flabellites steinkern terminology. L', W', T' are deformed counterparts of length L, width W, and thickness T in undeformed steinkerns. ρ and Φ are angular measures of strain. Other features mentioned in the text include impressions of the sulcus (S), fold (F), costae (C), cardinal process (CP), median septum (MS), hinge line (HL), and diductor muscle scar (DMS), as well as the approximate position of the hinge axis (HA).

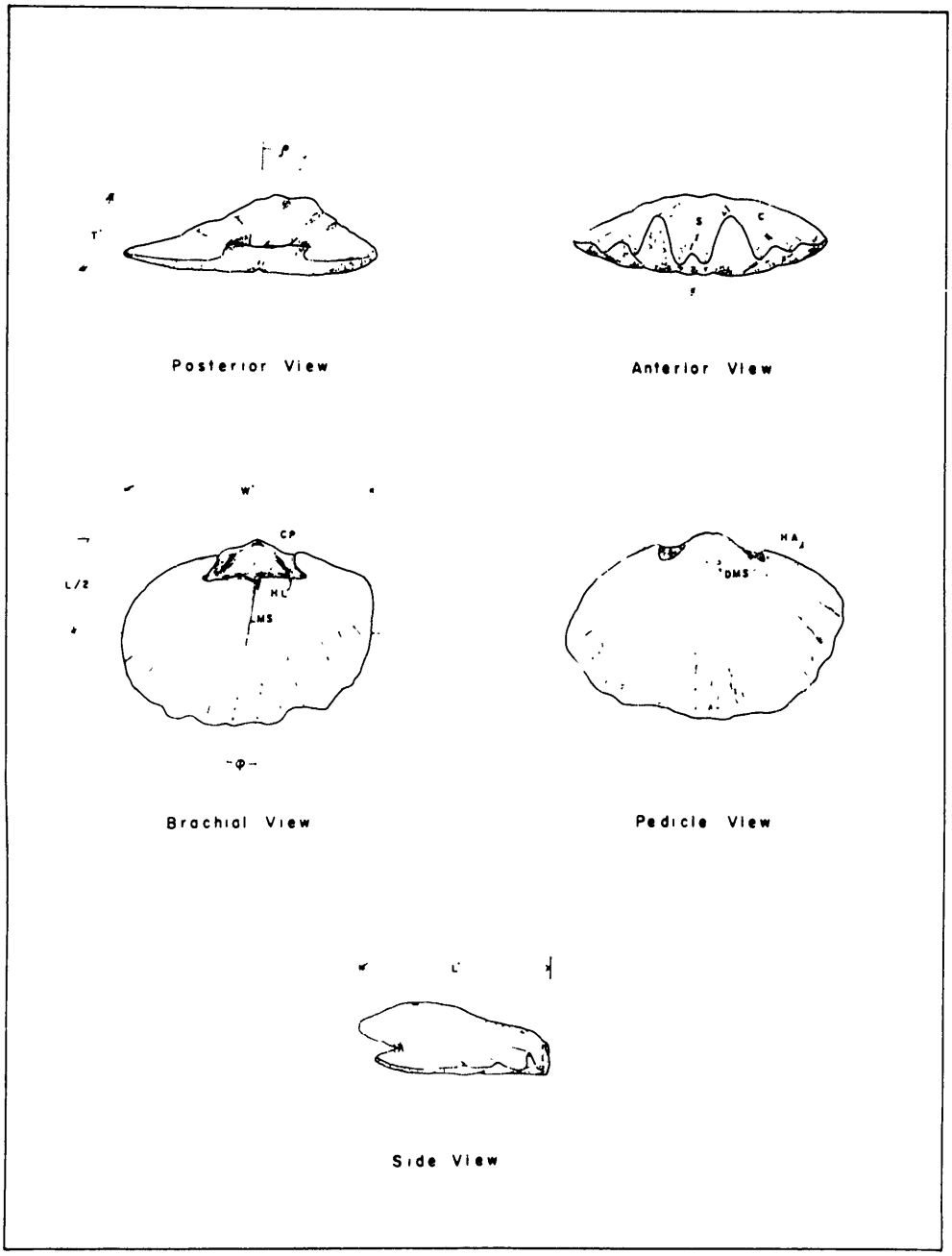
Posterior View
Anterior View
S
C
CP
HL
MS
L/2
Brachial View
HA
DMS
Pedicle View
Side View

a plane of bilateral symmetry perpendicular to the hinge axis and passing through the middle of the pedicle and brachial valves, as shown in Figure 2.

In life, the larger, convex pedicle valve was joined to the smaller, flat brachial valve by muscles internally attached to the posterior end of each valve on either side of a fulcrum-like structure. By contracting or relaxing the proper muscles, the valves rotated open or closed about a line in space, the hinge axis (Rudwick, 1959, p. 18). The hinge axis is approximately parallel to the hinge line which is the edge of a shelf protruding into the posterior of the brachiopod interior.

The area of attachment of a particular set of muscles, the diductors, are preserved as two small symmetric muscle scars on the pedicle valve, and as a protuberance on the brachial valve known as the cardinal process. This cardinal process passes anteriorly into the median septum, a small knife-like ridge usually coincident with the trace of the symmetry plane on the brachial valve.

The anterior and lateral edges of the steinkern are notched with mated saw-tooth crenulations caused by radial ribs, called costae, which ornament the brachial and pedicle valves. Where the symmetry plane crosses the anterior margin, it bisects a large crenulation which is expressed by a pronounced trough, or sulcus, on the pedicle valve and a corresponding fold, less pronounced, on the brachial valve.

After death, complete separation of pedicle from brachial valve is hindered by an internal, interlocking, tooth and socket mechanism, but the decay of the muscles permits the anterior margin to gape slightly and sediment sifts in to fill the shell interior. The sediment which accumulates inside the valves receives the detailed impression of all interior features including the muscle scars, cardinal process, median septum, and costae. This interior cast is the steinkern, the geologic strain gage used in this study.

Parameters. Strain is the deformation of shape. To measure strain in deformed Leptocoelia, certain dimensions and angles must be compared with their pre-deformation value.

In studying strain, as will be shown below, it is useful to measure three distances which were mutually perpendicular before deformation. The length, width, and thickness of Leptocoelia steinkerns are three such dimensions.

Length, denoted as L, is defined as the distance along that line formed by the intersection of the symmetry plane with the plane of the brachial valve, and included between perpendicular projections to this line of the anterior and posterior extremities of the steinkern. This distance is slightly shorter than the straight line distance between anterior and posterior extremities of the steinkern. See Figure 2.

Width, denoted as W, is defined as the distance between lateral edges of the steinkern in a direction parallel to the hinge axis and bisecting the length L. For steinkerns with one lateral edge damaged, it is assumed that the width W is equal to twice the distance between the remaining lateral edge and the median septum impression, measured parallel to the hinge axis as in undamaged specimens. See Figure 2.

The direction of W in deformed steinkerns must be determined with care. It is defined as parallel to the hinge axis, because the hinge axis is normal to the symmetry plane in undeformed specimens. Although the direction of the hinge axis is easily found in undeformed specimens, for deformed Leptocoelia it must be determined with less accuracy from the approximately parallel direction of the hinge line impression on the brachial posterior of the steinkern. Possible errors introduced by this approximation will be evaluated in a later section of this paper.

Thickness, denoted as T, is defined for undeformed steinkerns as the maximum distance between the brachial and pedicle sides of the steinkern measured in a direction perpendicular to the plane of the brachial valve. For deformed fossils, this distance must be multiplied by the secant of an angle ρ defined below and illustrated in Figure 2.

To fully describe strain, angle changes as well as changes in length must be measured. In general, the most

convenient angular changes are related to changes from the perpendicular of three lines which were mutually perpendicular before deformation, such as L, W, and T in this study.

The angle ρ is defined as the angle between the line formed by the intersection of the symmetry plane with the TW plane, and the normal to the plane of the brachial valve. It is measured by viewing the posterior of the steinkern normal to the TW plane and noting the angle between the brachial plane normal and a line passing through the median septum and the pedicle muscle scar as shown in Figure 2.

The angle φ, illustrated in Figure 2, is defined as the angle in the LW plane between the median septum and the normal to W.

Both ρ and φ are zero for undeformed steinkerns and, in special cases, for deformed specimens also. ρ and φ adequately define the angular change in two perpendicular planes, the TW and LW planes, but the morphology of Leptocoelia steinkerns does not permit accurate recognition of angular changes in the third perpendicular plane, the LT plane. Thus T, whose angular change is undefined in the LT plane, will always be too short by an amount proportional to (sec x-1) where x is the unmeasurable angle in the LT plane. However, because ρ and x should be the same order of magnitude, and because ρ is usually less than 10°, this factor is effectively zero (sec 10°)-1 = 1.015 - 1 $\approx$ 0 in most cases.

Growth curves. To measure strain, geometry before and after deformation must be known. For Leptocoelia steinkerns, five geometrical parameters L, W, T, ρ, and φ have been defined, but the pre-deformation values are known only for ρ and φ. ($\rho = \varphi = 0$ by definition for the unstrained state.)

Data for determining the ratios of any two of the parameters L, W, and T before deformation were obtained from collections of Leptocoelia flabellites from the Camden chert of Tennessee, from the Highland Mills member of the Esopus formation (Boucot, in preparation) at Highland Mills, N.Y., and from the Gaspe sandstone, eastern Gaspe, Quebec Province.

The Camden steinkerns were collected 60 years ago for the United States National Museum by Charles Schuchert from a 60 foot exposure of the Camden chert near Camden, Benton County, Tennessee (Saffard and Schuchert, 1899). At this locality, the formation is 275 feet thick, consisting mostly of thin-bedded, white to yellow chert containing abundant fossils whose details are preserved in unusual perfection (Dunbar, 1918, p. 751). Geologic structures are absent and the beds are nearly flat lying.

The slightly silicified steinkerns from the Highland Mills member of the Esopus formation were collected near the railroad station at Highland Mills, Orange County, New York. Here, faulting and some folding have deformed

the beds so that they now dip 60 degrees.

The Gaspe steinkerns were collected a half century ago by Shaler from the Gaspe sandstone somewhere in eastern Gaspe. The geology at the collecting locality is unknown to the writer, but regionally the Gaspe sandstone occupies the center of a broad syncline traversed by local faults and folds which occasionally impart vertical dips to the usually slightly inclined strata (McGerrigle, 1950).

L and T of all three collections are plotted as functions of W in Figures 3 and 4. The steinkerns measured (18 from the Camden chert, 14 from the Highland Mills member, and 40 from the Gaspe sandstone) represent the least damaged, best preserved specimens from the collections available.

Ratios obtained from the growth curves shown in Figures 3 and 4 are used in this study making the following assumptions: 1) Leptocoelia flabellites exhibited similar growth patterns irrespective of the time or place in which they grew, 2) these steinkerns have not been significantly deformed by diastrophism, 3) the compositional differences of the steinkerns do not significantly affect the final shape by variations in their reaction to physical or chemical diagenesis, 4) steinkerns from the Camden, Highland Mills, and Gaspe collections are individuals of the same species contained in rocks near the Tarratine railroad cut.

Assumption one is necessary because the collections

Figure 3. L vs. W for Camden, Highland Mills, and Gaspe Leptocoelia steinkerns. Straight line visually estimated from Camden steinkerns only, and only for size range of Tarratine steinkerns.

$$L = .78\,W + 1.20$$

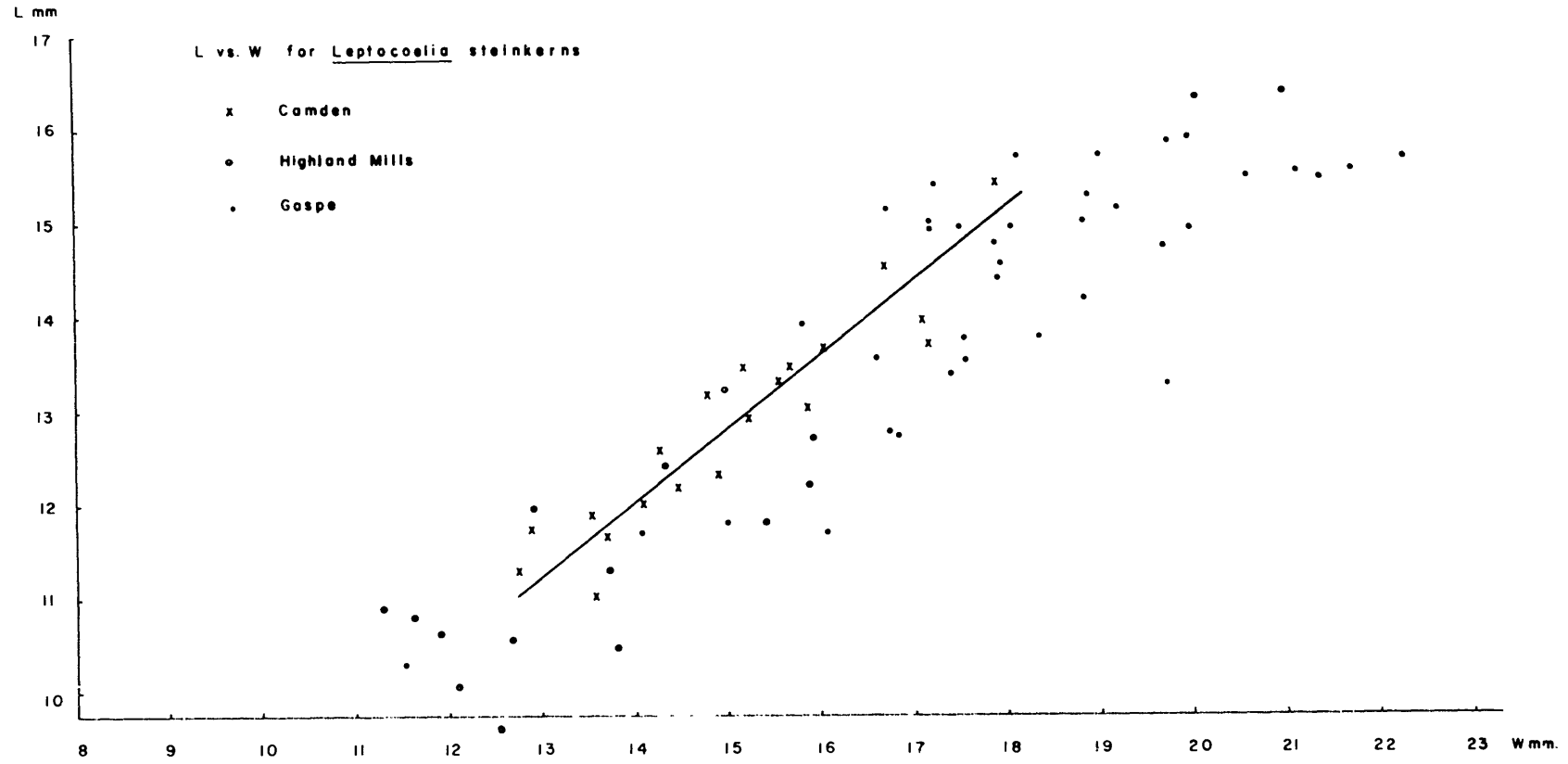
L mm
L vs. W for Leptocoelia steinkerns
x Camden
o Highland Mills
• Gaspe
17
16
15
14
13
12
11
10
8
9
10
11
12
13
14
15
16
17
18
19
20
21
22
23
Wmm.

Figure 4. T vs. W for Camden, Highland Mills, and Gaspe Leptocoelia steinkerns. Straight line visually estimated from Camden steinkerns only.

$$T = .30\,W + .28$$

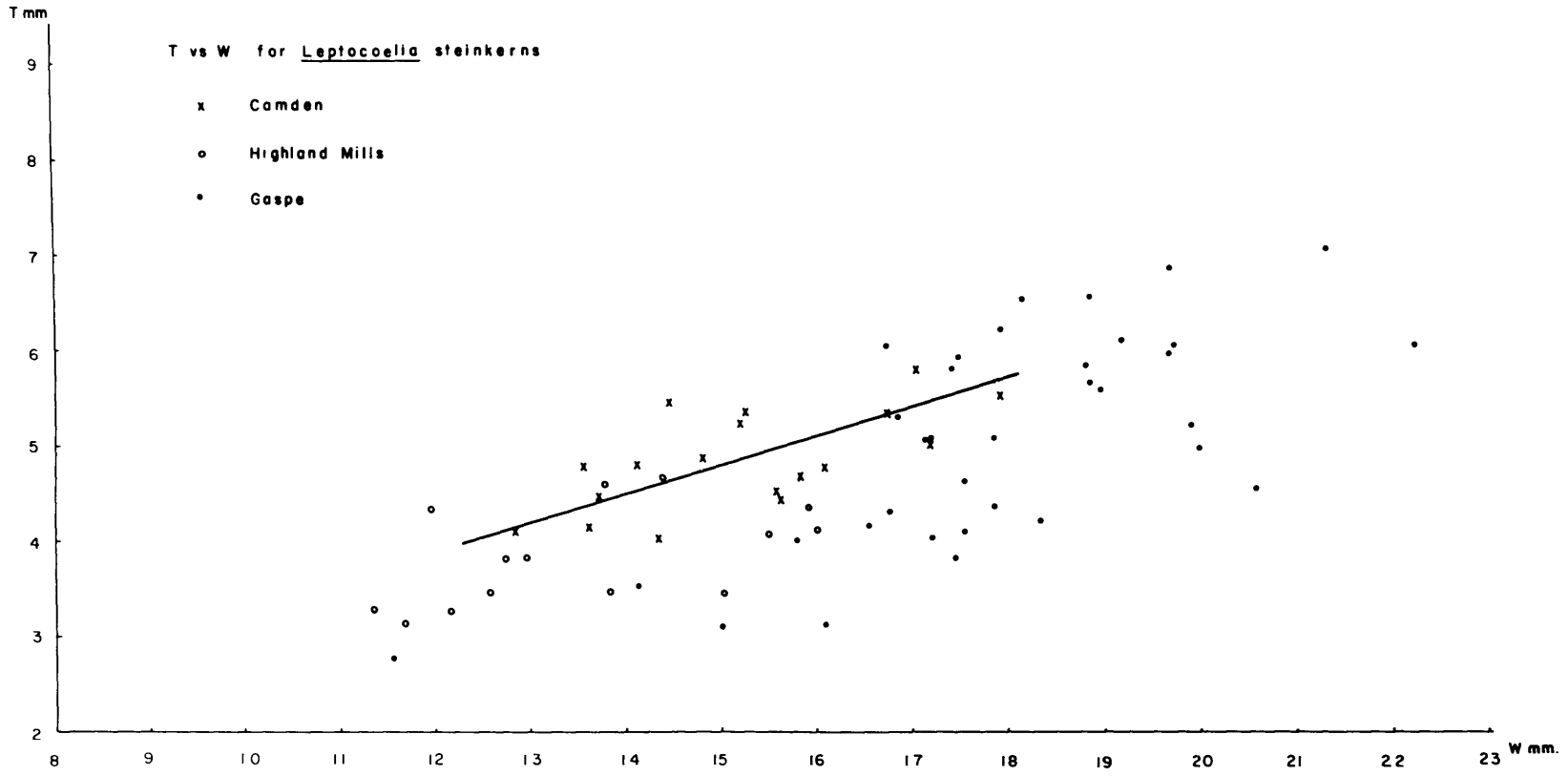
T mm
T vs W for Leptocoelia steinkerns
x Camden
o Highland Mills
• Gaspe
9
8
7
6
5
4
3
2
8
9
10
11
12
13
14
15
16
17
18
19
20
21
22
23
W mm.

from which the growth curves were constructed are widely separated geographically and temporally. The Tarratine Leptocoelia of Oriskany age are one fauni-zone older than the Esopus fossils from Highland Mills and the Gaspe, and three fauni-zones older than the Onondaga fossils of Camden (Boucot, personal communication, 1959).

The second assumption, that there has been no significant deformation due to diastrophism, is doubtfully valid for the Highland Mills fossils which were taken from steeply dipping rocks, and the Gaspe specimen whose exact, original geologic environment is unknown to the writer. For this reason, the straight lines in Figures 3 and 4 are based only on well preserved Camden steinkerns collected from the flat-lying rocks of western Tennessee.

Assumption three, equal reaction to diagenesis, is necessary because the Camden steinkerns are chert, the Highland Mills steinkerns are silicified medium sand, the Gaspe steinkerns are fine to medium sand, and the Tarratine steinkern are fine sand. Secondary growths of drusy quartz were noticed on Camden steinkerns.

Within the size range of Tarratine steinkerns, L and T are linear functions of W, but the largest steinkerns from the Gaspe (see Figure 3) show that the curve probably changes slope for large values of W, and the non-zero intercept of the straight lines (see equations on Figures 3 and 4) indicates that the slope of the curve must also change for

small values of W.

The non-zero intercepts of the linear relations shown in Figures 3 and 4 make exact determination of even the parameter ratios uncertain. For example, the slope of the L versus W line in Figure 3 is .78 anywhere along the line, but $^{L}/_{W}$ for any particular point on this line will vary exponentially along the straight line, approaching the value of the slope, .78, in the limit as the size of the steinkerns becomes impossibly large.

However, the change of parameter ratios is very small within the size range of Tarratine steinkerns. $^{L}/_{W}$ is probably between .855 and .900 and $^{T}/_{W}$ is probably between .315 and .330 for all Tarratine steinkerns used in this study. Because this variation is small compared to the variation imparted by strain, the growth curves in Figure 4 will be used to determine the pre-deformation ratio of any two of the strain parameters, L, W, and T, in the Tarratine steinkerns. Notice that without further assumptions, the growth curves determine only pre-deformation ratios, and not pre-deformation magnitudes of L, W, and T.

How these growth curves may be made to yield more information on the original shape of the steinkerns will be shown below in the section on strain.

Sample Collection and Preparation

Collection. Samples containing the deformed Leptocoelia steinkerns studied in this report were collected from the fossiliferous outcrops near Tarratine, Maine in the following manner.

Each fossiliferous outcrop was located on the fifty foot to the inch outcrop map previously prepared by Joyner and B. Boucot (1950). The exact location of each sample collected, and its position with respect to neighboring samples was established by a tape and compass survey.

On a suitable plane surface of the sample, an identification number, a horizontal line, and a line in the dip direction of the surface were marked with an acid-resisting marking pencil. The type of surface marked (cleavage, bedding, or joint), the position of the marked surface with respect to the sample (top surface or under surface), and the strike and dip of the marked surface were recorded.

Usually, one or more photographs of the outcrop were taken with a Polaroid Land camera, and the photograph immediately labeled with the sample number.

The sample was then freed from the outcrop with the aid of sledges, chisels, and a crow bar, and wrapped in newspaper. In anticipation of further research, many more samples were collected than are used in this report.

A 300 meter section of the lower Tarratine sandstone was described and measured. Orientation of bedding, cleavage, joints, and faults were recorded, and representative samples of the unfossiliferous beds were collected.

Preparation. In the laboratory, the oriented specimens were unwrapped, catalogued, and stored until needed. In preparing the steinkerns for measurement, the sample was first soaked in dilute hydrochloric acid for 8 hours to dissolve the calcareous shell material, then washed in running water for 8 to 12 hours to prevent deposition of iron salts in the rock, and then dried for at least twelve hours. Figure 5 shows the surface appearance of typical samples before and after treatment with acid.

Suitable steinkerns on the oriented surface of dried samples were exposed, but not extracted, with a vibra tool in preparation for the position measurements.

The following sections describe measurement of the position of a steinkern with reference to the oriented surface of the sample, and measurement of the magnitudes of L', W', T', ρ, and φ in an extracted steinkern. The goniometer used for position measurements, the strain gage used for dimension measurements, and the device used for measuring ρ and φ are all described and their use illustrated.

Figure 5. Top: typical sample after acid treatment, showing pedicle side of several steinkerns.

Lower left: typical sample before acid treatment.

Lower right: unpolished section of the untreated sample.

Position Data

Because part of the desired information is the orientation of principal strains in the structure from which the steinkerns were taken, it is necessary to keep track of position during sampling and extracting. This is done most conveniently with the aid of three coordinate systems.

The first of these coordinate systems is the geographic system established from the outcrop map, and tape and compass measurements. In this system, the locality of a fossiliferous sample is a point, and this point becomes the origin of a new system, the right-handed sample coordinates, in which the x axis is the horizontal strike line, the positive y axis is the dip line, and the positive z axis is the outward normal to the marked surface of the sample. A point in the sample coordinates becomes the origin for the third coordinate system, the steinkern coordinates, in which L', W', and T' form a right-handed, usually non-orthogonal system where positive L' extends toward the anterior of the steinkern.

The orientation of principal strains is first found in the steinkern coordinate system by use of Mohr diagrams described below. By referring the steinkern coordinates back through the sample coordinates to the geographic system, the orientation of principal strains is determined for a particular point in the deformed rocks southeast of

Tarratine. Because the geographic position is known from the outcrop map and tape and compass survey, and sample orientation is known from dip and strike measurements, this section deals only with determining the orientation of the steinkern coordinates L', W', T'.

Instrument description. To measure the position of L', W', and T', the large goniometer in Figure 6 was constructed. By the proper combination of translation and rotation, this goniometer determines the direction of any line in a sample less than 9 inches in maximum diameter.

The horizontal translating apparatus consists of an east-west track on which is mounted a north-south track. By motion in these perpendicular directions, any point in the sample can be brought to the center of the goniometer. A jack mounted on the north-south track provides vertical translation which brings the steinkern into the plane of the outer circle.

The outer circle, shown in Figure 6, is part of the rotational mechanism of the goniometer which also includes the semicircle, the head, and a vertical axis about which the jack can rotate. The outer circle is a graduated circle free to rotate about the vertical axis of the goniometer. Fixed to the outer circle and perpendicular to it is the semicircle on which the pointer and graduated dial of the head are located. The pointer in the head is free to rotate about its own long axis. A 3/4 inch needle is mounted

perpendicularly at the tip of the pointer (Figure 6). The vertical axis about which the jack rotates is actually a superfluous, but convenient degree of rotational freedom.

Measurement procedure. The prepared sample is placed on a sandbag resting on the jack, and the oriented face is leveled with the use of a line level. By translation on the east-west and north-south tracks, the sample is brought to the center of the goniometer. By rotation of the outer circle and/or rotation of the jack, the strike line on the leveled face of the sample is brought parallel with a loop of string stretched across the semicircle, as shown in Figure 6. Then the value of the outer circle at an index mark is recorded to the nearest degree, thus establishing the direction of the x axis in the sample coordinate system.

By translation, the exposed steinkern is brought to the center of the goniometer directly beneath the pointer. The steinkern is given an identification number. Next, its distance from the origin of the sample coordinates is measured in order to test strain homogeneity within the confines of a single sample. Then the relative position of the pedicle valve (up or down), and the approximate direction of the steinkern posterior (I, II, III, or IV quadrant of xy plane) in sample coordinates is recorded to remove an ambiguity which developes in the following measurements of undirected line segments.

Figure 6. Goniometer used to measure orientation of Leptocoelia steinkerns in sample. Size gage on right front of goniometer used to measure L', W', and T'.

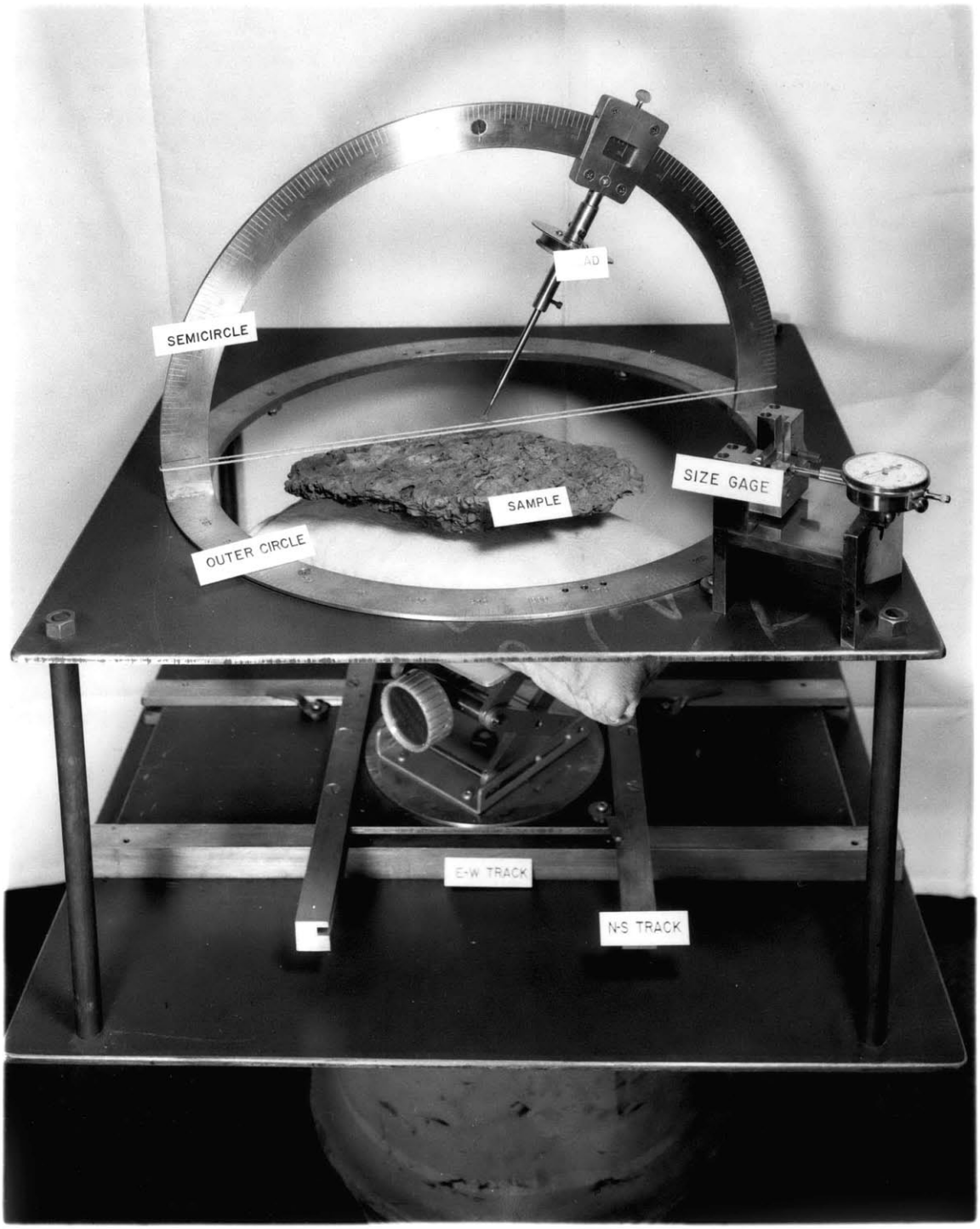
SEMICIRCLE
AD
SIZE GAGE
SAMPLE
OUTER CIRCLE
E-W TRACK
N-S TRACK

The needle is rotated into the plane of the semicircle, and by rotation of the outer circle it is brought parallel with the strike of L' in the steinkern. The angle between the x sample axis and L' in the steinkern is determined from the reading on the outer circle opposite the index mark. The dip of L' is determined by rotating the head over the semicircle until the needle parallels L' in space.

Exactly similar procedure is used to determine the dip and strike of W'. Occasionally, when steinkerns are oriented with their L'W' plane at high angles to the leveled surface of the sample, it is necessary to vary the procedure by rotating the needle and reading angles from the dial on the head.

On a stereonet, the dip and strike of L' and W' determine the L'W' plane and the approximate position of T', all with reference to known directions in the sample coordinate system. To check against large errors, the stereonet plot should be compared immediately with the orientation of the steinkern before it is extracted.

Strain Data

Once the position of the steinkern has been established, it is extracted from the sample by further drilling with the vibra tool and additional acid treatments if necessary. Extracted steinkerns are labeled in India ink

with their identification number and placed in individual boxes similarly numbered.

L', W', T' measurements. The dimensions L', W', and T' are measured with the size gage shown on the goniometer in Figure 6. The size gage consists of an Ames 282m dial gage mounted on a brass stand containing a sliding platform on which the steinkern is placed. For measuring L' and W', the gage is used as shown in Figure 6; for measuring T', the sliding platform is raised and the whole gage turned 90 degrees so that the side containing the platform is on the bottom. All dimensions are measured to the nearest .01 mm.

Following the definition of length given above on page 45, the L' dimension in the steinkern is measured parallel with a line scribed in the surface of the gage platform on which the steinkern rests. Because its direction is clearer from the brachial side, L' is measured with that side facing upwards.

Similarly, the dimension W' is measured with the brachial side facing upwards and with W' in a direction parallel with the line scribed on the platform. Because W' is probably the most difficult measurement to take, it is best obtained by averaging several readings.

After turning the size gage on its side, T' is measured from the steinkern, laid brachial side up, on the platform block.

ρ and φ measurements. The steinkern is mounted on plasticene in a 4x3x1 inch cardboard sample box in such a way that the L'W' or T'W' plane lies parallel with, and just below the top of the box.

To standardize the measurement of ρ and φ, wire loops having the same center line were clamped 4 and 8 inches above the base of a ring stand and directly in line with the steinkern. Angles are measured by sighting through the loops at the intersection of a protractor and clear plastic straight edge laid across the top of the box parallel with the appropriate directions in the steinkern.

THEORY

Definition

From the parameters L, W, T, ρ, and φ and the growth curves in Figures 3 and 4, it is desired to find the magnitudes and directions of the axes of the strain ellipsoid. The best way to get the required information from the available data is to use as strain components the quadratic elongation λ, and the unit shear γ (Nadai, 1950, p. 117).

The quadratic elongation λ is the square of the ratio of the length of the line r' in the strained state to its length r in the unstrained state. Since the square root of quadratic elongation $\sqrt{\lambda}$ is the length of a line from the center to the surface of the strain ellipsoid, the semi-axes of the strain ellipsoid are labelled $\sqrt{\lambda}_1$, $\sqrt{\lambda}_2$, and $\sqrt{\lambda}_3$ where $\lambda_1 > \lambda_2 > \lambda_3$. The unit volume change, K, in terms of the strain axes is

$$(1) \qquad \sqrt{\lambda_1 \lambda_2 \lambda_3} - 1 = K.$$

The unit shear γ is the tangent of ψ, where ψ is the angle between a direction in the strained state and the normal to the strain ellipsoid for that direction. Where the angle ψ lies in a principal plane of the strain ellipsoid, it is the complement of the angle in the strained state between two lines originally perpendicular in the unstrained state (Jaeger, 1956, p. 21).

The use of λ and γ in describing finite strain in Leptocoelia implies that the strain ellipsoid does not vary in magnitude or direction over a volume at least as large as an individual steinkern. In the present study, this kind of finite homogeneous deformation will be simply called strain.

The use of γ and λ to describe a strained state, and its graphical representation using the Mohr diagram was developed by Nadai (1950, pp. 117-129), and is summarized by Jaeger (1956, pp. 34-38). Brace (in preparation) illustrates the application of the Mohr diagram to finding the principal strain axes for the case of plane strain in deformed fossils, pebbles, crystals, and cross-bedding.

The method used below in analyzing strain in Leptocoelia steinkerns is based on the previous work of Nadai, Jaeger, and Brace. It is assumed that the reader knows the content of these studies.

A list of symbols used in this paper are included in an appendix.

Mohr Diagrams

Strain in any given direction can be completely described by the appropriate λ and γ, but it is ordinarily very difficult to understand from just an ordered pair of numbers how strain in the given direction is related to strain in the entire body. For this reason, graphical

representation of finite strain by a Mohr diagram is particularly useful.

A particular state of strain can be graphically represented in two interdependent ways: 1) the Mohr diagram for the unstrained state, and 2) the Mohr diagram for the strained state.

Mohr diagram for the unstrained state. In the Mohr diagram for the unstrained state, strain in any direction is represented by image points within two closed regions of the λ , γ plane whose boundaries are three ellipses of the form:

$$(2) \qquad \frac{\left(\lambda - \frac{\lambda_i + \lambda_j}{2}\right)^2}{\left(\frac{\lambda_i - \lambda_j}{2}\right)^2} + \frac{\gamma^2}{\left(\frac{\lambda_i - \lambda_j}{2\sqrt{\lambda_i \lambda_j}}\right)^2} = 1$$

$$i,j = 1,2,3$$
$$i \neq j$$

Each of the three ellipses represents strain in one of the three principal planes of the strain ellipsoid. If deformation on a principal plane has been accomplished without area change in that plane, that is, if $\lambda_i \lambda_j = 1$, then the Mohr ellipse for that plane becomes a circle.

Each image point on the Mohr diagram for the unstrained state indicates the position of a line before strain, and the amount of deformation which the line has undergone

during strain. The direction cosine, ℓ_i, of the line in the unstrained state can be found by solving two equations of the form:

$$(3)\quad \ell_i^2 = \frac{\lambda_i (\lambda - \lambda_j)(\lambda - \lambda_k) + \gamma^2}{\lambda (\lambda_i - \lambda_j)(\lambda_i - \lambda_k)}$$

$$i,j,k = 1,2,3$$
$$i \neq j \neq k \neq i$$

Equation (3) represents a series of non-concentric ellipses in the variables λ and γ which reduce to one of the principal ellipses in equation (2) when $\ell_i = 0$. The curve $\ell_i = 0$ represents directions in a principal plane of the strain ellipsoid. From image points on the curve $\ell_i = 0$, direction cosines can be determined graphically (Nadai, 1950, p. 126).

The amount of deformation is the λ , γ coordinates of the point. λ varies from a maximum of λ_1 to a minimum of λ_3. γ varies from a maximum

$$(4)\quad \gamma_{max} = \frac{\lambda_i - \lambda_j}{2\sqrt{\lambda_i \lambda_j}}$$

to a minimum of zero in the directions of the three principal strain axes.

Mohr diagram for the strained state. An image point on the λ , γ plane indicates the position of a line before

strain, but in deformed Leptocoelia, it is the position of the line after strain that is more easily determined. To show the relationship of lines after strain, the Mohr diagram for the strained state is used.

By the transformation

$$(5) \qquad \lambda' = \frac{1}{\lambda} \quad ; \qquad \gamma' = \frac{\gamma}{\lambda}$$

the ellipses of the form of equation (2) map into circles of the form

$$(6) \qquad \left(\lambda - \frac{\lambda_i' + \lambda_j'}{2}\right)^2 + \gamma^2 = \left(\frac{\lambda_i - \lambda_j}{2}\right)^2$$

the Mohr diagram for the strained state is the graphical representation of such circles on the λ', γ' plane.

The direction cosines of an image point on the λ', γ' plane are given by curves, $l_i' =$ constant, passing through the given point concentric about the centers of principal circles. Direction cosines before and after strain are related by the formula:

$$(7) \qquad l_i = l'_i \sqrt{\frac{\lambda}{\lambda_i}} \qquad \text{(Nadai, 1950, p. 119)}$$

Mohr Diagrams Applied to Leptocoelia Steinkerns

Initial information. Given enough information, Mohr diagrams can be derived which completely describe the position and deformation of any line in a deformed body. For Leptocoelia steinkerns, the initial information consists

of two angles ρ and φ whose unstrained values are zero, three lengths L', W', T' whose undeformed dimensions L, W, T have the following ratios:

$$(8) \qquad \frac{L}{W} = .87, \quad \frac{T}{W} = .32, \quad \frac{T}{L} = .37;$$

and finally the growth curves in Figures 3 and 4.

The three possible combinations of angular changes between L', W', and T' in a deformed steinkern have been schematically illustrated in Figure 7. In the most general case (Figure 7a), no pair of lines will remain perpendicular after deformation; in a less common case (Figure 7b), two pairs of lines will still be at right angles following strain; and in the extraordinary case (Figure 7c), all three pairs of lines will exhibit no angular change.

The most general case where no pair of lines remains perpendicular after deformation does not seem to give enough initial information for readily obtaining Mohr diagrams. The extraordinary case where all three lines remain perpendicular after deformation will occur only when L', W', and T' are parallel with the strain axes. In Leptocoelia steinkerns, this rare case could not be differentiated from the second case, where only two line pairs remain perpendicular, because the angular change x in the LT plane is unmeasurable. Because the first case contains insufficient information and the third case is indistinguishable from the second, the theory was developed for deformed

Figure 7. Possible angle changes resulting from the deformation of 3 mutually perpendicular lines A, B, C.

(a) general case, no pair of lines remain perpendicular

(b) less common case, 2 pair of lines remain perpendicular

(c) extraordinary case, 3 pair remain perpendicular

This study is restricted to case (b). Note that it is impossible to have only one pair of lines remain perpendicular after strain.

Before strain

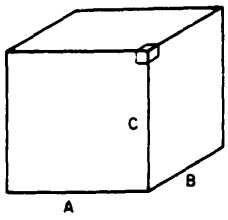

3 right angles

(a) After strain

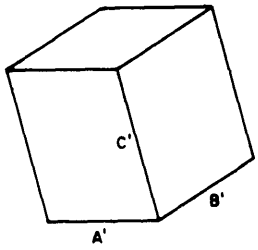

No right angles

(b) After strain

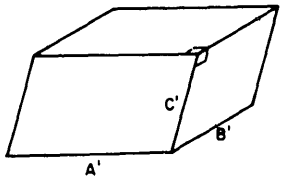

2 right angles

(c) After strain

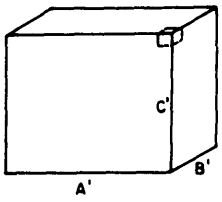

3 right angles

steinkerns where either ρ, or φ, or ρ and φ are zero. Whenever only one of the angles ρ or φ is zero, it must be assumed that the unmeasurable angle x is also zero, for it is impossible that only one of the three line pairs remains perpendicular after strain.

In deformed Leptocoelia steinkerns containing two pairs of perpendicular lines (Figure 7b), the line common to both pairs must parallel one of the principal strain axes. The direction of this principal axis in the rock will have been previously determined from position measurements described above.

Partial or complete identification of the strain axis is possible by comparing the ratios $\frac{L'}{W'}$, $\frac{T'}{W'}$, $\frac{T'}{L'}$ with their undeformed counterparts in equation (8) and using the algebra of inequalities to obtain the relative values of the elongations $_A = (\frac{A'}{A})^2$ (A = L, W, or T). The various possibilities are represented in the following scheme.

$$\sqrt{\lambda_A} > \sqrt{\lambda_B} > \sqrt{\lambda_C} \qquad (A,B,C = L,W,T)$$

if $\sqrt{\lambda_A}$ is a strain axis, it is either $\sqrt{\lambda_1}$ or $\sqrt{\lambda_2}$
if $\sqrt{\lambda_B}$ is a strain axis, it must be $\sqrt{\lambda_2}$
if $\sqrt{\lambda_C}$ is a strain axis, it is either $\sqrt{\lambda_2}$ or $\sqrt{\lambda_3}$

Thus without recourse to a Mohr diagram, the direction and the partial or complete identity of a strain axis is known.

Strain on λ', γ' plane. The remaining two strain axes lie in the plane of the steinkern containing the non-perpendicular line pair A'B' (A',B' = L',W',T'). The

departure from the perpendicular of this line pair is an angle whose tangent is the γ coordinate of λ_A and λ_B on the λ, γ plane. From the transformation in equations (5), γ_{AB} is also the slope of the line on the λ', γ' plane,

$$(9) \qquad \gamma' = \gamma_{AB} \lambda' \qquad (A,B = L,W,T).$$

The exact value of λ_A and λ_B are unknown, but measurements of A' and B', combined with the appropriate ratio from equations (8) yield the new ratio

$$(10) \qquad \frac{\lambda'_A}{\lambda'_B} = \frac{\lambda_B}{\lambda_A} = \left(\frac{A}{A'}, \frac{B'}{B}\right)^2 = f' \qquad (A,B = L,W,T).$$

By assuming an arbitrary value for λ'_B, solving equation (10) for λ'_A, and solving equation (9) for γ'_A and γ'_B, two points on a principal circle of the λ', γ' diagram are known. By drawing the circle containing these points, the ratio

$$(11) \qquad \frac{\lambda'_i}{\lambda'_j} = g' \qquad (i \quad j),$$

and the direction cosines of A' and B' can be graphically determined.

From the transformation of equations (5), it can also be seen that maximum shear, γ_{max}, on a principal plane is the slope of a line passing through the origin and tangent to all circles with a radius $\frac{\lambda'_j - \lambda'_i}{2} = \frac{\lambda'_j(1 - g')}{2}$.

γ_{max} is thus a straight line envelope of a family of curves including the arbitrary circle determined by the choice of λ'_B, and the unique circle describing strain on a principal plane of the given deformed steinkern. Because both arbitrary and unique circles are numbers of a family with a straight line envelope passing through the origin, direction cosines and the dimensionless ratio g' determined from the arbitrary circle will be identical to those in the unique circle.

Determination of principal strains. The initial information includes pre-deformation ratios of steinkern parameters, measurements of a particular steinkern, and the direction and relative magnitude of one strain axis. By use of the Mohr diagram for the strained state, the initial information yields the ratio, g', of the remaining principal strain axes, the direction cosines ℓ_i' of the steinkern parameters with respect to these two axes, and the value of γ_{max} on the principal plane containing these two axes. In what follows, this initial and derived information will be used to obtain the magnitudes of the three principal strain axes and the approximate directions of the two strain axes whose positions are yet unspecified.

The expression for γ_{max} on a principal plane (equation (4)) is related to the ratio g' by the following equation:

$$(12) \quad \gamma_{max} \equiv \frac{\lambda_i - \lambda_j}{2\sqrt{\lambda_i \lambda_j}} = \frac{1 - g'}{2\sqrt{g'}}$$

γ_{max} is thus a function of g' only which, on the λ , γ plane, means it is the horizontal envelope to all ellipses having a given g' and the form of equation (2).

It now becomes a problem to fix which, of all the possible ellipses determined by γ_{max}, is the unique ellipse describing strain on a principal plane in a deformed Leptocoelia steinkern. Determining the unique ellipse becomes possible by expressing the strain state in terms of steinkern parameters and by introducing an initial condition in the form of the growth curves on Figures 3 and 4.

By using equation (7) each principal strain axis can be given in terms of the elongation of one of the parameters L, W, or T, and the direction cosines of the parameter before and after straining.

$$(13) \quad \sqrt{\lambda_i} = \frac{\ell'_i}{\ell_i} \sqrt{\lambda_A} \qquad \begin{matrix} A = L,W,T \\ i = 1,2,3 \end{matrix}$$

By substituting equation (13) into equation (1) and rearranging terms, the following important relation results:

$$(14) \quad LWT = \frac{\ell'_1 \ell'_2 \ell'_3}{\ell_1 \ell_2 \ell_3} \quad \frac{L'W'T'}{1 + K}$$

In this equation, L', W', and T' are known measured values; the direction cosine ratio for the parameter parallel to a strain axis is unity; and the direction cosines of A' and B'

in the strained state are determined graphically from their image points on the λ', γ' plane.

It remains to determine the direction cosines in the unstrained state of the non-perpendicular line pair A'B' used in equation (10). From the auxiliary definition of γ given above on page , these two direction cosines must be equal, and the image points representing A' and B' on the λ, γ plane must have the ordinate value γ_{AB} and lie on a principal ellipse. This would be enough information to determine the missing direction cosines if all the curves on the Mohr diagram were circles instead of ellipses.

However, the abscissas of these points will be determined by the shape of the principal ellipse on which they lie. For a given γ_{max} or g', the shape of any ellipse depends on a shape factor $\frac{1}{\sqrt{\lambda_i \lambda_j}}$, which is the ratio of vertical to horizontal semi-axes. The relations between $\frac{1}{\sqrt{\lambda_i \lambda_j}}$, and the shape and identity of the resulting ellipse are included in Table II.

The first two columns of Table II show the relation of the magnitude of the shape factor to the shape of the resulting Mohr ellipse on the λ, γ plane. The third column identifies the Mohr ellipse for different ranges of the shape factor. These relations, which follow from equations (1), (2), and (4), are usually valid for most strain states, and are rigorously valid when volume change, K, is zero.

Table II The relation between $\frac{1}{\sqrt{\lambda_i \lambda_j}}$, and ellipse shape and identity on λ, γ' plane, assuming K = 0.

magnitude of shape factor	shape of Mohr diagram	identity of Mohr diagram
$\frac{1}{\sqrt{\lambda_i \lambda_j}} < 1$	γ'_{max} minor ellipse axis	$\lambda_1 \lambda_2$ plane, or $\lambda_1 \lambda_3$ plane if $\lambda_2 < 1$
$\frac{1}{\sqrt{\lambda_i \lambda_j}} > 1$	γ'_{max} major ellipse axis	$\lambda_2 \lambda_3$ plane, or $\lambda_1 \lambda_3$ plane if $\lambda_2 > 1$
$\frac{1}{\sqrt{\lambda_i \lambda_j}} = 1$	γ'_{max} radius of circle	$\lambda_1 \lambda_3$ plane

From the previous studies of strain in fossils and ooids listed in Table I, a rough idea of the quantitative influence of the factor $\frac{1}{\sqrt{\lambda_i \lambda_j}}$ can be gained. Taking Cloos' average value of principal strains as typical, the values of this factor are 1.45, 1.05, and .66 at constant volume.

From these values, it is apparent that the major ellipse on the λ, γ' plane will be close to a circle, as long as the strain ellipsoid does not approach a rotational solid. Thus the direction cosines of image points on this major ellipse can be determined by assuming the ellipse is a circle.

For the intermediate and minor ellipses, greater departures from circularity are evident, but possibly direction cosines of image points with low δ' ordinates can also be measured from an approximating circle. For Tarratine steinkerns, the strain is relatively low and the departure from circularity is correspondingly lower than the typical values of Cloos.

With some uncertainty, the two remaining direction cosines are thus determined, and equation (14) becomes a relation between (LWT) and volume change, K. By assuming a volume change, (LWT) can be computed from equation (14). From Figure 8, the computed value of (LWT) yields a specific W, and from Figures 3 and 4, this W locates L and T.

These operations yield $\sqrt{\lambda}_L, \sqrt{\lambda}_W, \sqrt{\lambda}_T$, one of which is a principal strain axis, and all of which have known directions in the rock. From equation (13) the magnitudes of the two remaining principal strains can be computed, and their directions in the rock obtained from the direction cosines of A' and B' on the λ', δ' diagram. Because the construction of Mohr eliminates the sign of the direction cosines, there are two possible positions for the location of these remaining principal strains, but this mathematical ambiguity can be resolved by observing which direction is consistent with the deformation in the steinkern.

Figure 8. LWT vs. W for size range of typical Tarratine steinkerns. This plot is a portion of the curve represented by the cubic equation:

$$LWT = .23\ W^3 + .58\ W^2 + .34\ W$$

This equation is derived from the straight lines drawn for Camden steinkerns in Figure 3 and Figure 4.

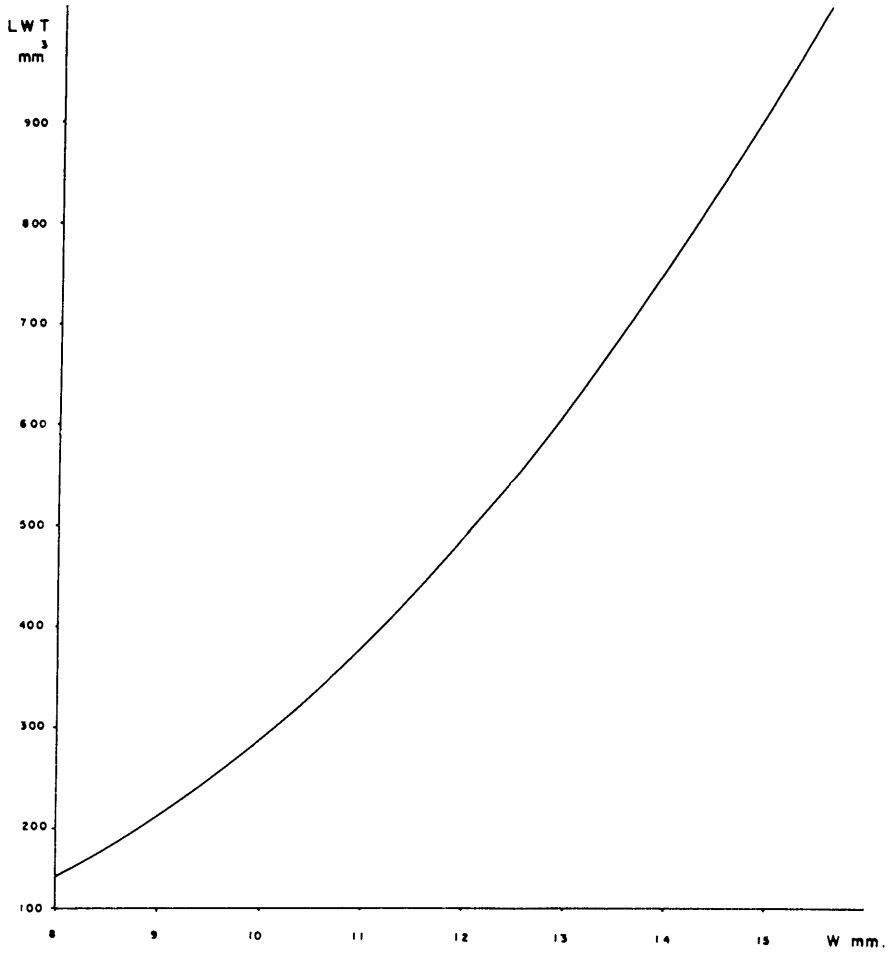
LWT
mm³
900
800
700
600
500
400
300
200
100
8
9
10
11
12
13
14
15
W mm.

Summary of strain determination in Leptocoelia steinkerns. The above presentation of the theory used in determining strain in Leptocoelia steinkerns is here briefly reviewed.

The initial information includes the measured parameters of a deformed steinkern, and the parameter ratios and growth curves of undeformed steinkerns. By specializing the type of deformation considered, the direction and partial identity of a principal strain axis is also known.

From this initial information, the shear, γ_{AB}, and the ratio of elongations, f', are determined for the two non-perpendicular directions A' and B' in the steinkern. These points, plotted on the Mohr diagram for the strained state, lead to the graphical determination, in the principal plane containing A' and B', of the maximum shear γ_{max}, the ratio of two principal strain axes g', and the direction cosines of A' and B' with respect to these axes.

This information is then applied to the λ, γ plane to obtain the approximate direction cosines of A' and B' in the unstrained state.

The strain state in terms of steinkern parameters gives a relation (equation (14)) in which the unknowns are the product (LWT) and the volume change K. By assuming a volume change, (LWT) is determined. The growth curves

(Figures 3 and 4) give an initial condition relating (LWT) to W (Figure 8). From Figure 8, the computed value of (LWT) locates W, and from Figures 3 and 4, W locates L and T.

These derived values of L, W, and T, and the measured values of L', W', and T' give three elongations, including a principal strain axis, of known direction in the rock. The remaining principal axes can be computed, and their directions located from the Mohr diagram for the strained state. Ambiguity of direction is removed by observing which of the two possible directions is consistent with the deformation in the steinkern.

RESULTS

Strain in Leptocoelia Steinkerns

Principle strains. The theory developed above suffers from a major drawback; it is based on a type of deformation which is comparatively rare. Of 24 steinkerns extracted from three samples, only two approximately satisfied the required angular relations shown in Figure 7b. Principal strains derived from these two steinkerns are shown on a lower hemisphere stereonet plot in Figure 9a. The plane of Figure 9 is the horizontal plane with north at the top of the figure. The location of samples in the field are shown on Plate I inside the rear cover.

The directions of the principal strains determined from both steinkerns are roughly similar. In both cases, the maximum and minimum strain axes lie nearly in the cleavage plane and the intermediate axis is at a high angle to the cleavage plane. The maximum axes are more nearly in the b direction, and the least strain axes are approximately in the a direction. Strain in the two steinkerns have approximately the same magnitudes.

Parameter elongation. However the majority of steinkerns fall into the general case of deformation illustrated by Figure 7a, and for these steinkerns, it seems that principal strains cannot be computed. Yet this case of deformation does give some information on strain. As indicated above (p. 76), relative elongations in the directions of L', W', and T' can be rigorously determined by comparison of deformed and undeformed parameter ratios.

Figure 9. a) principal strains in C3

b) elongations in sample C2A, C3, and C5A. Values for C3 are underlined.

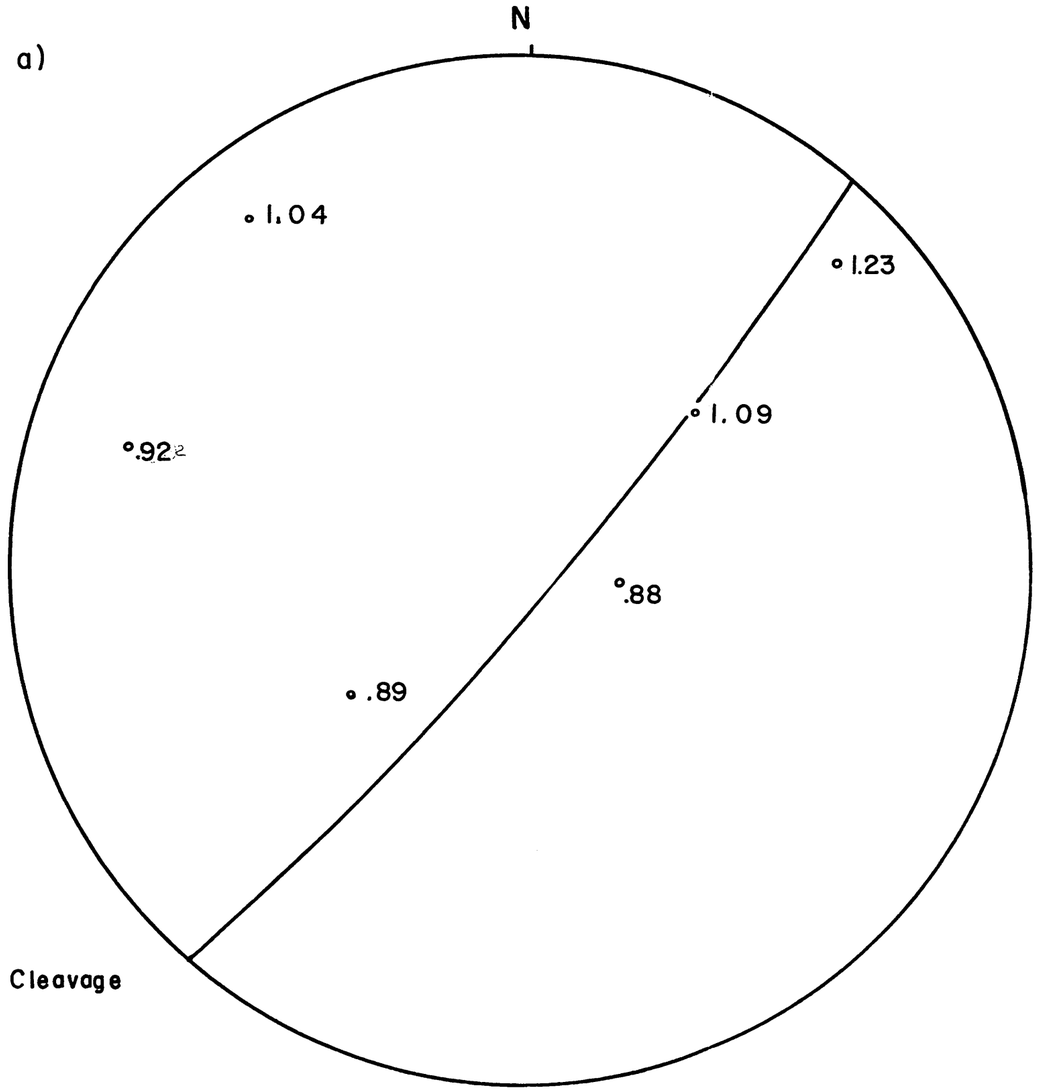
a)
N
1.04
1.23
1.09
.92
.88
.89
Cleavage

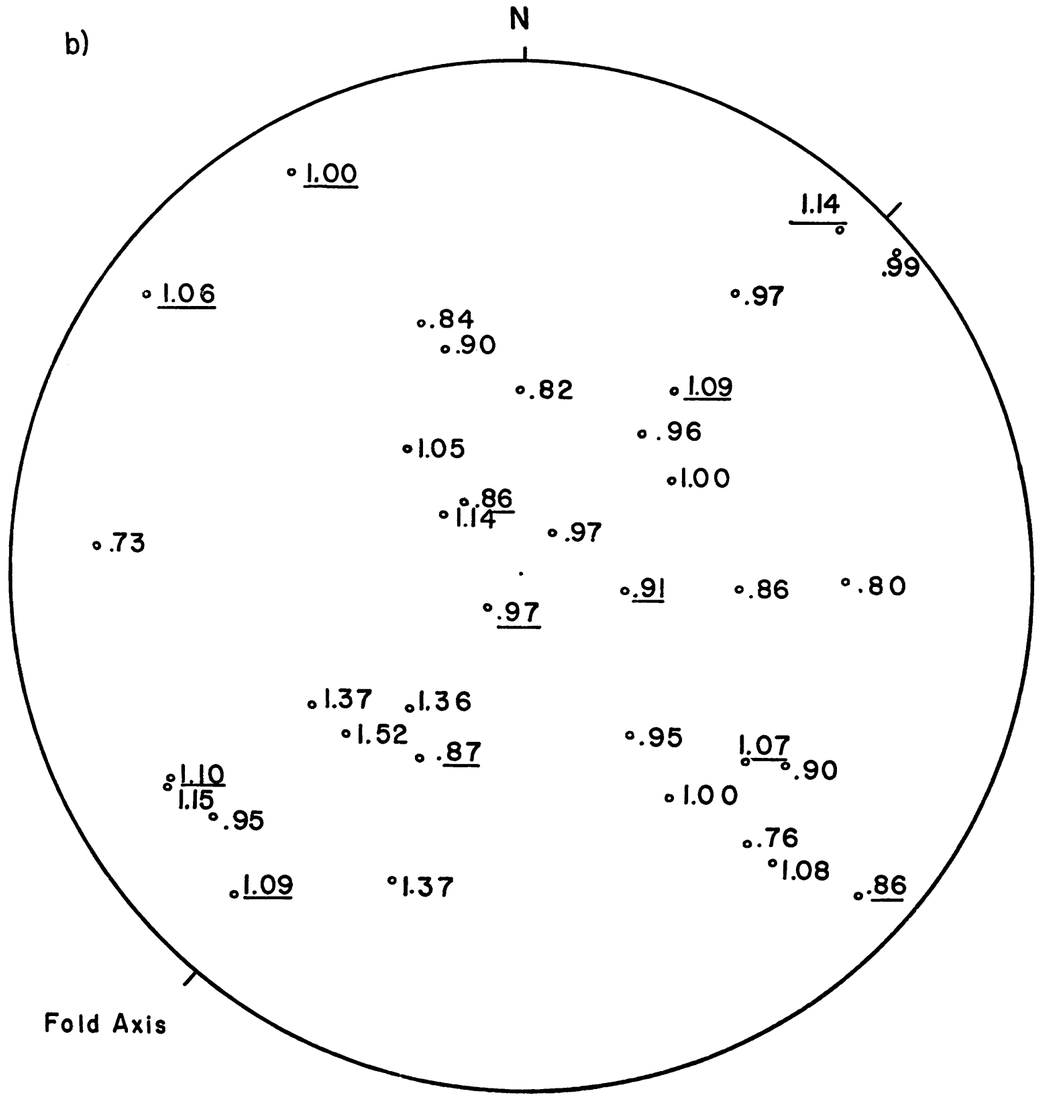
b)
N
1.00
1.14
.99
1.06
.97
.84
.90
.82
1.09
.96
1.05
1.00
.86
1.14
.97
.73
.91
.86
.80
.97
1.37
1.36
1.52
.95
1.07
.90
.87
1.10
1.15
.95
1.00
.76
1.08
1.09
1.37
.86
Fold Axis

By plotting relative elongations for L^1, W^1, and T^1 of each steinkern as 1, 2, or 3 on a stereonet, it should be possible to define the direction of principal strains from the areas on the net where 1 and 3 have their respective maxima. To do this, a great many steinkerns must be measured, and the results only give directions of principal strains.

The absolute magnitude of elongations in the directions of L^1, W^1, and T^1 might be determined from equation (14) if the direction cosine term could be evaluated. From trial cases for imaginary strain states having principal strains with the same order of magnitude as on Figure 9a, it seems that this term usually has a value very close to 1. Qualitatively, this is reasonable because each direction cosine relates L^1, W^1, or T^1 to λ_1, λ_2, or λ_3 in such a way that the ratio $\frac{\ell_1^1}{\ell_1}$ which is greater than one is partially compensated for by the ratio $\frac{\ell_3^1}{\ell_3}$ which is less than one.

By assuming that the direction cosine term does equal one, and by assuming that volume change is zero, a very simple relation is obtained from equation (14).

$$(15) \qquad (LWT) \approx L^1W^1T^1$$

From this relation, elongations of L, W, and T can be computed by using Figure 8, and Figures 3 and 4 in the manner explained above (p. 86).

Table III lists the parameter elongations for 12 steinkerns from three samples. The elongations of parameters for sample C3 shown by the underlined numbers on Figure 9b

Sample Number	L^I	W^I	T^I	ρ	ϕ	λ_L	λ_W	λ_T	λ_1	λ_2	λ_3
C3-3	12.73	13.34	5.18	5.5°R	0	1.00	.91	1.10	1.23	.92	.88
C3-7	12.42	11.36	4.53	13.0°R	4.0°L	1.09	.86	1.07			
C3-9f	16.40	15.45	5.97	2.5°L	0	1.09	.87	1.06	1.09	1.06	.88
C3-11f	11.92	11.00	3.15	5.0°R	2.5°L	1.19	.97	.86			
C2A-3	12.03	14.40	7.20	12.5°L	14.0°L	.86	.84	1.36			
C2A-4	11.41	11.23	3.28	14.0°R	6.0°L	1.15	1.00	.90			
C2A-5	13.40	11.45	6.80	20.0R	8.0°R	1.00	.73	1.37			
C2A-6	12.05	13.83	8.35	4.0L	18.0°L	.82	.80	1.52			
C5A-1	15.42	15.28	4.51	10.0°R	7.0°L	1.14	.97	.90			
C5A-2	15.07	17.11	5.96	12.0°L	15.0°L	.99	.95	1.05			
C5A-3	14.86	13.93	7.89	11.5°L	12.5°L	.96	.76	1.37			
C5A-4	13.05	15.60	5.51	13.0°R	5.5°L	.95	.97	1.08			

TABLE III. Measurements of deformed Leptocoelia steinkerns. Relative values of λ_L, λ_W, and λ_T are correct, but except for C3-3 and C3-9f, numerical values are approximations from a simplified form of equation (14), $LWT \approx L^I W^I T^I$. Location of samples shown in Plate I inside rear cover.

indicate the same type of deformation shown by the principal strains derived from C3 in Figure 9a.

Elongations from C2A and C5A, Figure 9, show greater scatter, but definitely indicate that the maximum strain axis dips 45° to the southwest, a direction which is at a high angle from the λ_1 indicated for C3. The elongations in C2A and C5A have maximum values 1.37 and 1.52, again in contrast to C3 which has a maximum λ of 1.24.

Sample C2A and C3 are on the same stratigraphic horizon 15 meters apart and 10 meters above the horizon containing sample C5. TableIV sums up the deformation characteristics of each of these samples. Averages of ρ and ϕ for C2A, C3, and C5A are based on 5, 6, and 4 steinkerns respectively.

TABLE IV. Deformation characteristics of C2A, C3, and C5A.

	Cleavage in steinkerns	λ_{max}	λ_{min}	ρ_{AV}	ϕ_{AV}
C2A	Yes	1.52	.73	9°	12°
C3	No	1.24	.86	5°	2°
C5A	Yes	1.37	.76	11.5°	10°

Comparison with previous work. The magnitude of strains shown on Figure 9 is of the same order of magnitude as the strain obtained by Breddin, Cloos, and Hellmers, as shown in Table I, but the direction of these strains is very unlike those obtained in previous studies of fossil deformation. The tendency of λ_1 to fall in a is not typical of strain in fossils, and the indication that λ_2 is in c, if verified by future work, is certainly unusual.

The scatter of values for steinkerns within each sample is typical of results reported in previous work, and the difference in deformation between samples has often been noted, although possible not over such small distance. The fact that elongations obtained from such an approximate relation as equation (15) still show a roughly consistent distribution within each sample indicates that strain is homogeneous within volumes less than a cubic meter, but the difference between samples shown by Table IV indicate strain is not homogeneous for volumes tens of cubic meters in extent.

Analysis Of Errors

Experimental errors. In this investigation, two classes of measurements have been made: measurements of position and measurements of strain data.

Position measurements are measurements of the dip and strike of L^1 and W^1 in a defined steinkern. In ten measurements of one steinkern, the strike of L^1 had a range of 5°, the dip of L^1 had a range of 9°, the strike of W^1 had a range of 4°, and the dip of W^1 had a range of 4°. These measurements were taken on the exposed brachial side of the steinkern, the easier side to measure.

Strain measurements include measurements of L^1, W^1, T^1, ρ, and ϕ. In ten measurements of C2A-3 (Table III), the standard deviation, s, is .14 mm for L^1, .20 mm for W^1, .22 mm for T^1, 1.5° for ρ, and 1.4° for ϕ. This shows that whatever is being measured, is being measured with ahigh degree of accuracy.

A study of damaged steinkerns indicates that breakage on the edge of the L^1W^1 plane may give measured values of L^1 and W^1 3 to 7% lower than their true value.

Theoretical assumptions. It is universally assumed that finite strain in rock components can be described by the strain ellipsoid. Yet the assumption is almost universally demonstrated to be invalid by the same authors who assume it. Almost every author who has investigated stretched pebbles describes their shape as lenticular, parallel sided, sword, paddle, cigar, or canoe shaped (Elwell, 1955, p. 80; Flinn, 1955, p. 486; Brace, 1955, p. 131; Kvale, 1945; Strand, 1944, p. 18; Turner, 1957, p. 10; and others). Pictures of stretched ooids by Chapmen (1893), Heim (1921), and Cloos (1947) conclusively demonstrate a non-elliptical outline for these features. This writer has observed that the edges of deformed Leptocoelia steinkerns are occasionally extended in paper-thin sheets.

If so called "flow" in rocks is not a misnomer, a lenticular or lemniscate outline of pebbles is logical to expect. Chorley (1959) notes numerous examples where this shape is imparted to an object immersed in a flowing fluid.

However, this study makes the usual assumption that deformation is approximated by a strain ellipsoid. The difference between elliptical and lenticular outlines is very slight for the low magnitudes of strain encountered in this study.

The second basic assumption in studies of finite strain in rock components is that strain in the fossil, ooid, or pebble is homogeneous, that is, the magnitude and directions of the principal strains

do not change within the particular geologic strain gage. For steinkerns in this study there is no reason to doubt this assumption because rectilinear features such as casts of costae, the median septum, and the hinge line have remained rectilinear in deformed steinkerns from the folded rocks of Tarratine.

Whether or not the region of strain homogeneity extends across the calcite shell separating the steinkern from the surrounding rock determines whether or not strain in the steinkern is representative of strain in the entire rock. An example where strain is not homogeneous across a fossil boundary is shown by a sample of quartzite supplied by J. B. Thompson in which the exterior of a circular calcite crinoid columnal was deformed to an ellipse, while the circular quartzite filling of the axial canal remained circular. Only two crinoid columnals have been found in the samples from Tarratine, but neither of them indicate that such inhomogeneous deformation has occurred there. Strain concentration in the thinner, fibrous shells of Leptocoelia is even less likely that in thick, single crystal crinoid columnals.

Note that the word 'homogeneous' is mathematically defined, and it implies nothing about the composition of the deformed material.

Application of the theory of finite homogeneous strain led to equations (14) and (15) which necessitated an assumption of volume change, K. $K = 0$ is probably a good assumption if the rock was lithified before deformation. Thin sections of the Tarratine sandstone do not show crushed and splintered quartz grains which might be expected if deformation took place before lithification. Pettijohn (1957) and Weller (1959) review studies of volume change in sediments, and

Rubey (1930) studied volume change in deformed shales, but reliable information on volume change in sandstone due to deformation is lacking.

Uncertainty in determining direction cosines in the unstrained state for use in equation (14) is discussed above on page 81. The assumption that the direction cosine term equals one in equation (15) was tested for a strain state with principal strains 1.4, 1, .7, which are the magnitudes of strain axes indicated by C2A and C5A (Figure 9). This trial showed that elongations computed from equation (15) will be too large, but probably not more than 10% too large, and the error will be proportional to the amount of shear in the L^1, W^1, and T^1 directions.

In using equations (14) and (15), it is necessary to assume that the growth curves on Figures 3 and 4 truly describe the original shape of Tarratine steinkerns. If this is so, the dimensions L^1, W^1, and T^1 should plot on these graphs as a straight line, more diffuse, but identical in slope and intercept to that line derived from Camden steinkerns. Plots of T^1 against W^1 and L^1 against W^1 for 60 Tarratine steinkerns showed that this requirement is satisfied by the T^1W^1 plot, but the L^1W^1 plot produced a line with a steeper slope.

If it can be assumed that no significant preferred orientation was imparted to the LW plane of the fossils at deposition, maximum elongations in the L^1W^1 ought to be equally distributed between the L^1 and W^1 directions. But Table III shows that $\lambda_{W'}$ which is derived from the growth curves, is never a maximum in the steinkerns encountered so far.

Both these facts, the steeper L^1W^1 line, and the low elongations

in the W' direction, indicate that one of the assumptions on which the use of the growth curves is based must be wrong (p. 49). Possibly there were environmental influences which resulted in local variations in Leptocoelia growth characteristics. However, the departure from the growth curves is not great, and the error introduced is small as indicated by the strains in Table III.

SUMMARY

Conclusions

The unequivocal testimony of diastrophism offered by deformed fossils, ooids, and pebbles has long excited the interest of geologists. Provided their original shapes and their field orientation are known, these geologic strain gages quantitatively describe the magnitudes, directions, and distribution of strain in deformed rocks.

Previous studies of strain in rocks indicate that the magnitude of quartzite pebble deformation usually far exceeds the strains recorded in fossils and ooids, and that the direction of maximum extension in pebbles is usually parallel with fold axes, while in fossils and ooids, maximum extension is perpendicular to fold axes, or equal to the intermediate strain.

For deformation in pebbles and ooids it is relatively simple to compute principal strains, but in fossils which lack an original spherical geometry, deformation could usually be measured only by assuming part of the information which was sought.

From Nadai's graphical representation of strains on the Mohr diagram, and a knowledge of a particular fossil's growth curve, it is possible to derive principal strains from deformed specimens of that fossil. This method has been applied to deformed steinkerns of the brachiopod, Leptocoelia flabellites, from folded rocks near Tarratine, Maine, but it is applicable to any fossil in which three mutually perpendicular directions can be recognized before deformation, and in which at least two of these directions remain recognizable after deformation.

Principal strains from two steinkerns showed that the intermediate strain axis is directed perpendicular to the cleavage plane and that the maximum strain axis is directed approximately parallel with the fold axis.

Approximate elongations in the directions of steinkern parameters were computed from 12 steinkerns. Parameter elongations in eight steinkerns from two samples about 20 meters apart indicated that maximum extension, as high as 1.5 dipped 45° in the axial plane of the fold. From a third sample parameter elongations in four steinkerns, including the two used for principal strain determinations, indicated that maximum extension as high as 1.2 lay along the horizontal fold axis. This third sample lay 15 meters along strike from one of the first two. The data from parameter elongation also suggests that the intermediate strain axis is perpendicular to cleavage. The difference in strain for samples a few tens of meters apart indicates that strain is not homogeneous for volumes across distances of this magnitude, but the approximately consistent magnitude and direction of elongations within each sample indicates that strain is homogeneous across distances on the order of tens of centimeters.

Suggestions for Future Work

This study is a preliminary investigation for the purpose of devising a suitable procedure to determine strain from Leptocoelia steinkerns. By a combination of biologic data and strain theory it has been possible to determine principal strains, and future work will concentrate on applying this method to oriented Leptocoelia

steinkerns collected from known positions on the folded rocks near Tarratine. From such a study may come a better understanding of the magnitude, orientation and distribution of strain developed in folded rocks.

As a by product of this study, several interesting problems have developed. From the constant angle between cleavage and bedding on the minor folds near Tarratine, it seems that cleavage may have developed before the minor folds, but further work is needed to support this. The apparent correlation between shell beds and a position above or in fine grained clastic material may give information on the paleoecology of Tarratine seas. The growth curves indicate that there may be distinct, measurable differences among individuals of the species Leptocoelia flabellites which may be correlated with their geographic origin.

Strain measurements in the steinkern should be correlated with petrofabric studies of quartz in the Tarratine sandstone and calcite in the shell material. An attempt should be made to develop a method to determine principal strains directly from the general case of a deformed steinkern with no remaining right angles.

BIBLIOGRAPHY

Barrande, J., 1852, Systeme Silurien du centre de la Boheme: plates.

Billings, M.P., 1954, Structural Geology: New York, Prentice-Hall, Inc., 514 pp.

Billings and Sharp, 1937, Petrofabric study of fossiliferous shist: Am. Jour. Sci., v. 34, pp. 277-292.

Boucot, A.J., MacDonald, Milton, and Thompson, 1958, Metamorphosed Middle Paleozoic fossils from central Massachusetts, eastern Vermont, and western New Hampshire: Geol. Soc. America Bull., v. 69, pp. 855-870.

Boucot, A.J., in preparation, Brachiopods of the Lower Devonian rocks at Highland Mills, New York.

Boucot, A.J., in preparation, Geology and paleontology of the Moose River synclinorium, northwestern Maine: U.S. Geol. Survey, Prof. Paper.

Boucot, A.J., Brace, W., and DeMar, R., 1958, Distribution of brachiopod and pelecypod shells by currents: Jour. Sed. Petrology, v. 28, pp. 321-332.

Brace, W.F., 1955, Quartzite pebble deformation in central Vermont: Am. Jour. Sci., v. 253, pp. 129-145.

Brace, W.F., in preparation, Use of Mohr circles in the analysis of large geologic strain.

Breddin, H., 1956a, Die Tektonishe Deformation der Fossilien im Rheinischen Schiefergebirge: Z. deutsch. geol. Ges., v. 106, pp. 227-305.

Breddin, H., 1956b, Tektonische Gesteinsdeformation im Karbongurtel Westdeutschlands und Sud-Limburgs: Z. deutsch. geol. Ges., v. 106, pp. 232-260.

Breddin, H., 1957, Tektonische Fossil - und Gesteindeformation im Gebiet von St. Goarshausen (Rheinisches Schiefergebirge): Decheniana, v. 110, pp. 289-350.

Bucher, W.H., 1953, Fossils in Metamorphic Rocks: Geol. Soc. America Bull., v. 64, pp. 275-300.

Chapman, F., 1893, On oolitic and other limestones with sheared structure from Ilfracombe: Geol. Mag., new. ser., v. 10, pp. 100-104.

Chorley, R.J., 1959, The shape of drumlins: Jour. of Glaciology, v. 3, no. 25, pp. 339-344.

Cloos, E., 1937, Interpretation of the crystalline rocks of Maryland: Geol. Survey Maryland, no. 13.

Cloos, E., 1947, Oolite deformation in the South Mountain fold, Maryland: Geol. Soc. America Bull., v. 58, pp. 843-918.

Conrad, T., 1841, Fifth Annual Report on the Paleontology of the State of New York: New York Geol. Survey fifth annual report, pp. 25-57.

Crickmay, C.H., 1933, Some of Alpheus Hyatt's unfigured types from the Jurassic of California: U.S. Geol. Survey, Professional Paper 175-B, pp. 51-64.

Daubree, G.A., 1876, Experiences sur la shistosite des roches et sur les deformations des fossiles correlatives de ce phenomene: Bull. Soc. Geol. France, 3rd series, v. 4, p. 529.

Daubree, A., 1879, Etudes synthetiques de geologie experimentale: Paris, Dunod, 828 pp.

Dawson, Sir J.W., 1855, Acadian Geology: Oliver & Boyd, Edinburgh, 388 pp.

De la Beche, H.T., 1829, Sketch of classification of the European rocks: Phil. Mag., v. 6, pp. 440-450.

Dufet, H., 1875, Note sur les deformations des fossiles contenus dans les roches shisteuses et sur la determination de quelques especes: Annoles scient de l'Ecole Normale Super. (Paris)(2 series) t. 4, p. 183.

Dunbar, C., 1918, Stratigraphy and correlation of the Devonian of western Tennessee: Am. Jour. Sci. 4th series, v. 46, pp. 732-756.

Elles, G.L., 1944, The identification of graptolites: Geol. Mag., v. 81, pp. 145-158.

Elwell, R.W.D., 1955, The lithology and structure of a boulder-bed in the Dolradian of Mayo, Ireland: Geol. Soc. London Quart. Jour., v. 111, pp. 71-81.

Fairbairn, H.W., 1949, Structural petrology of deformed rocks: Cambridge, Addison Wesley Press, Inc., 344 pp.

Flinn, D., 1956, On the deformation of the Funzie conglomerate, Fetlar, Shetland: Jour. Geol., v. 64, pp. 480-505.

Haughton, S., 1856, On slatey cleavage and the distortion of fossils: Phil. Mag., v. 12, pp. 409-421.

Hall, J., 1859, Paleontology of New York, v. 3: New York Geol. Survey, 532 pp.

Heim, Alb., 1878, Untersuehen uber den Mechanismus der Gebirgsbildung: 2 Bde. u. 1 Attas - Basel, Schwabe.

Heim, Alb., 1919 u. 1921, Geologie der Schweiz Band I. Molasseland & Juragebirge; Band II: Die Schweizer Alpen, Leipzig, Tauchnitz.

Hellmers, J.H., 1955, Krinoidenstielglieder als Indikatoren der Gesteinsdeformation: Geol. Rundshaw, v. 44, pp. 87-92.

Hitchcock, Edward, 1835, Report on the geology, mineralogy, botany, and zoology of Massachusetts, 2d ed., Amherst, 702 pp. and Atlas.

Hitchcock, E., Hitchcock, C.H., and Hager, A.D., 1861, Report on the geology of Vermont, 2 vols., Claremont, N.H., 988 pp.

Imlay, R., 1939, Upper Jurrassic ammonites from Mexico: Geol. Soc. America Bull., v. 50, p. 26.

Jaeger, J.C., 1956, Elasticity, fracture, and flow: New York, John Wiley and Sons, Inc., 152 pp.

Jannettay, E., 1884, Memoir sur les clivages des roches (shistosite, longrain): Soc. Geol. France Bull., 3d ser. v. 12, pp. 211-236.

Johnson, W.R., 1936, The ostracoda of the Missouri series in Nebraska: Neb. Geol. Survey, paper no. 11, 52 pp.

Kvale, A., 1945, Petrofabric analysis of a quartzite from the Bergsdolen quadrangle, western Norway: Norsk. Geol. Tidskr., v. 25, pp. 193-215.

Lake, P., 1943, Restoration of the original form of distorted specimens: Geol. Mag., v. 80, pp. 139-147.

Lardy, C. (1832), Sur les belemnites de la Nuffenen: Actes Soc. helvetique des Sci. Nat., p. 92.

Loretz, H., 1882, Uber transversal-schieferung und verwandte Erscheinungen in Thuringischen Schiefergebirge: Jahrb. Preuss. Geol. Landesanstalt. 1881, pp. 258-306.

McGerrigle, 1950, The geology of eastern Gaspe: Quebec Province of Mines Geol. Rept. 35.

Mehnert, K.R., 1938, Die Meta-Konglomerate in sachsischen Erygebirge: Min. pet. Mitt., Bd 50, pp. 194-272.

Nadai, A., 1950, Theory of flow and fracture of solids: New York, McGraw-Hill Book Co., 572 pp.

Oftedahl, C., 1948, Deformation of quartz conglomerates in central Norway: Jour. Geol., v. 56, pp. 476-487.

Pettijohn, F.J., 1934, Conglomerate of Abram Lake, Ontario and its extensions: Geol. Soc. America Bull., v. 45, pp. 479-506.

Pettijohn, F.J., 1957, Sedimentary rocks, 2nd ed., New York: Harper and Brothers, 718 pp.

Phillips, J., 1844, On certain movements in the parts of stratified rocks: Rpt. 13th meeting of the British Assoc. for the Advancement of Science. Cork, 1843. Notices and abstracts of miscellaneous communications to the sections, 1844, p. 60.

Rubey, W.W., 1930, Lithologic studies of fine-grained Upper Cretaceous sedimentary rocks of the Black Hills region,: U.S. Geol. Survey Prof. Paper 165A, pp. 34-38.

Rudwick, M., 1959, Growth and form of brachiopod shells: Geol. Mag., v. 96, p. 1.

Runner, J.J., 1934, Pre-Cambrian geology of the Nemo District, Black Hill, South Dakota: Am. Jour. Sci., 5th ser., v. 28, pp. 353-372.

Rutsch, F.R., 1949, Die Bedentung der Fossil-deformation: Bull. Ass. Swisse geol. petro., v. 15, pp. 5-18.

Safford, J., and Schuchert, C., 1899, The Camden chert of Tennessee and its lower Oriskany fauna: Am. Jour. Sci., 4th series, v. 7, pp. 429-432.

Sharpe, D., 1847, On slatey cleavage: Proc. Geol. Soc., v. 3, pp. 74-105.

Sharpe, D., 1849, On slatey cleavage, II, : Proc. Geol. Soc., v. 5, p. 111.

Sieburg, R., 1909, Uber transversale Schieferung im Thuringischen Schiefergebirge: Z. Prakt Geol., v. 17, pp. 233-262.

Sorby, H.C., 1853, On the origin of slatey cleavage: New Philos. Jour. (Edinburgh), v. 55, pp. 137-148.

Sorby, H.C., 1879, The Anniversary Address of the president: Quart. Jour. Geol. Soc. London, v. 35, p. 39.

Sorby, H.C.S., 1908, On the application of quantitative methods to the study of the structure and history of rocks: Geol. Soc. London Quart. Jour., v. 64, p. 71.

Strand, T., 1938, Nordre Etnedal, Norges Geol. Unders. Beskr. Geol. Gradteigskart, no. 152, 71 pp.

Strand, T., 1944, Structural petrology of the Bydgin conglomerate: Norsk geol. tidsskrift, v. 24, pp. 14-31.

Turner, F.J., 1957, Linneation, symmetry, and internal movement in monoclinic tectonite fabrics: Geol. Soc. America Bull., v. 68, pp. 1-18.

Wanner, A., 1890, Casts of Scolithus flattened by pressure: American Geol., v. 5, pp. 35-38.

Weller, J.M., 1959, Compaction of Sediments: American Assoc. Petroleum Geol., v. 43, pp. 273-310.

Wettstein, A., 1886, Uber die Fischfauna des tertiaren Glarnerschiefers. Abh. d. Schweiz. pal. Ges., v. 13, 101 pp.

APPENDIX

List of Symbols

a	dip direction in cleavage
b	strike of cleavage, or fold axis
c	direction perpendicular to cleavage
f'	ratio of elongations on a principal plane
g'	ratio of principal strains on the plane containing f'
i, j, k	subscripts 1, 2, 3 in any order
ℓ_i	direction cosines in unstrained state referred to λ_i
ℓ_i'	direction cosines in strained state referred to λ_i'
r	length of line before deformation
r'	length of same line after deformation
s	standard deviation
x	unmeasureable angle in $L'T'$ plane
x	direction parallel with strike line on sample
y	direction in dip line of sample
z	direction perpendicular to xy plane
A, B, C	parameters L, W, T in any order
K	volume change
L	length of steinkern
T	thickness of steinkern
W	width of steinkern
L', W', T'	L, W, T in deformed steinkerns; also fossil coordinates
γ	shear, the tangent of ψ
ψ	angle between a radius vector to the surface of the strain ellipsoid and the normal to the ellipsoid at that point

λ quadratic elongation $\left(\frac{r'}{r}\right)^2$

λ_1, λ_2, λ_3 principal strains ($1 > 2 > 3$)

λ_L, λ_W, λ_T elongation in direction of L', W', and T'

λ_A, λ_B, λ_C elongations of L', W', T' in any order

ρ complement of angle between T' and W'

ϕ complement of angle between L' and W'

Plate I

OUTCROP MAP AND CROSS SECTION OF LOWER TARRATINE FORMATION

EAST OF TARRATINE, MAINE

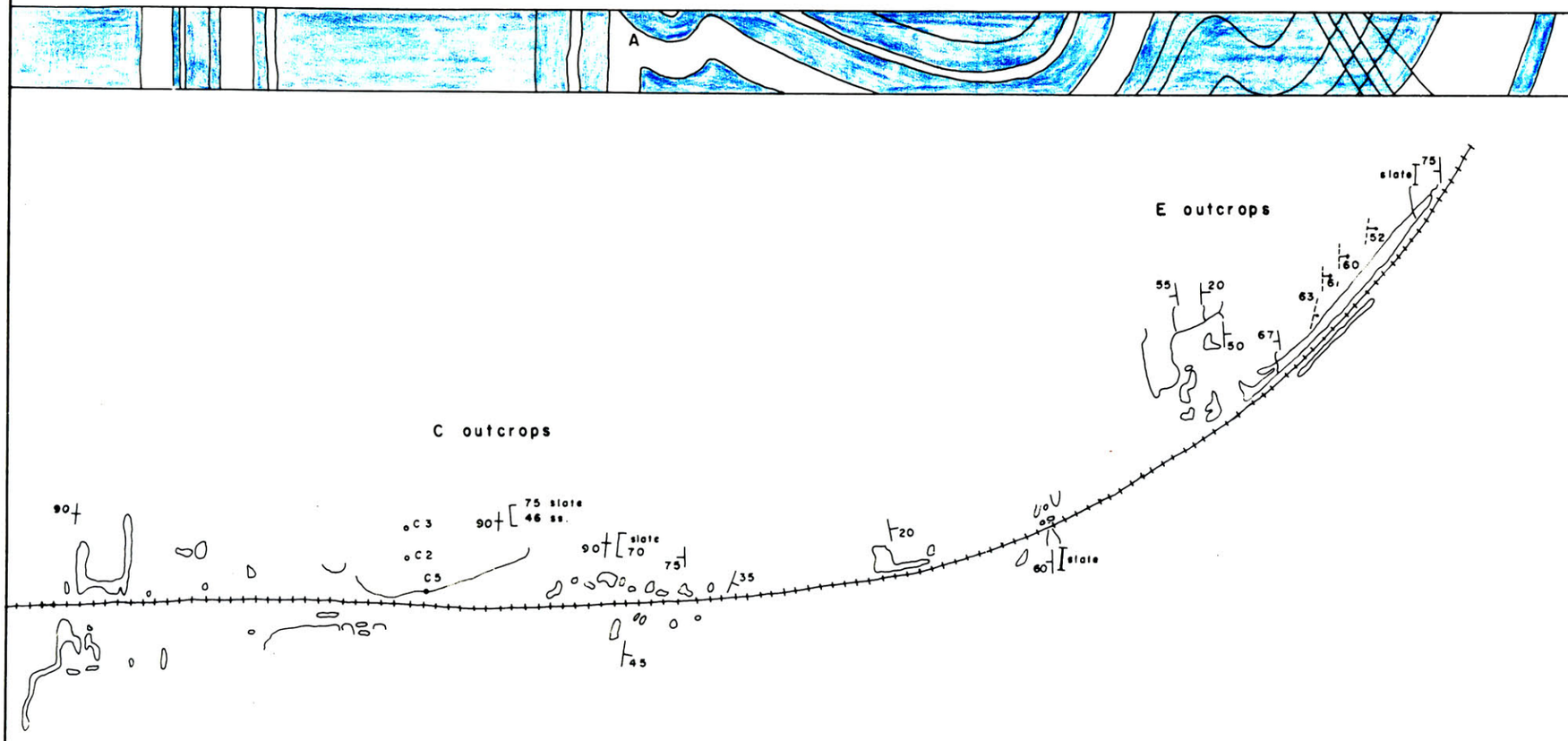

From Joyner and B. Boucot, 1950

INDEX MAP

• Tarratine, Maine

LEGEND

- Attitude of bedding (31)
- Attitude of cleavage (78)
- Attitude of faults (52)
- Sandstone with less than 20% slate & siltstone
- Covered
- Area of outcrop
- Sample locations

SCALE

0 100 200 300 400 Feet

True North